FINAL REPORT

FABRICATION, CHARACTERIZATION, AND THERMAL CONDUCTIVITY
OF POROUS COPPER AND STAINLESS STEEL MATERIALS

/ by

Gerald Friedman
WHITTAKER CORPORATION/NUCLEAR METALS DIVISION

prepared for

NATIONAL AERONAUTICS AND SPACE ADMINISTRATION

NASA - Lewis Research Center
Contract NAS3-13309
Anthony Fortini, Project Manager

FINAL REPORT

FABRICATION, CHARACTERIZATION, AND THERMAL CONDUCTIVITY
OF POROUS COPPER AND STAINLESS STEEL MATERIALS

by

Gerald Friedman

WHITTAKER CORPORATION/NUCLEAR METALS DIVISION
Concord, Massachusetts

prepared for

NATIONAL AERONAUTICS AND SPACE ADMINISTRATION

September 1970

Contract NAS3-13309

NOTICE

This report was prepared as an account of Government sponsored work.
Neither the United States, nor the National Aeronautics and Space Admin-
istration (NASA), nor any person acting on behalf of NASA:

A.   Makes any warranty or representation, expressed or implied, with
      respect to the accuracy, completeness, or usefulness of the in-
      formation contained in this report, or that the use of any informa-
      tion, apparatus, method, or process disclosed in this report may
      not infringe privately owned rights; or

B.   Assumes any liabilities with respect to the use of, or for damages
      resulting from the use of any information, apparatus, method or
      process disclosed in this report.

As used above, "person acting on behalf of NASA" includes any employee
or contractor of NASA, or employee of such contractor, to the extent that
such employee or contractor of NASA, or employee of such contractor
prepares, disseminates, or provides access to, any information pursuant to
his employment or contract with NASA, or his employment with such con-
tractor.

Requests for copies of this report should be referred to

        NASA Scientific and Technical Information
          Facility
        P. O. Box 33
        College Park, Maryland   20740

FOREWORD

TABLE OF CONTENTS

ABSTRACT

Spherical high-purity copper and stainless steel powders were isostatically compacted into bodies of 10, 20, and 30 percent porosity. Representative samples were used to characterize the parts with respect to chemical analysis, pore geometry, and thermal and electrical conductivity. The parts were determined to be of highly uniform porosity, both within each sample and from sample to sample.

FABRICATION, CHARACTERIZATION, AND THERMAL CONDUCTIVITY OF POROUS COPPER AND STAINLESS STEEL MATERIALS

by

Gerald Friedman
WHITTAKER CORPORATION/NUCLEAR METALS DIVISION

SUMMARY

Stainless steel and copper parts of 10, 20 and 30 percent porosity were manufactured by isostatic compaction techniques from closely sized spherical metal powders. Porosity was characterized by means of bulk measurements, mercury intrusion, and metallographic techniques and was found to be highly uniform within the parts and from part to part. Thermal and electrical conductivity measurements were made for each material at each porosity level, in vacuum, from room temperature to 700°F (371°C) for copper and to 900°F (482°C) for stainless steel.

INTRODUCTION

One of the basic properties needed in the design of transpiration cooled structures is the thermal conductivity of the body in the form in which it is being used. Porous bodies are being considered as cooling surfaces in such self-cooled structures. Because there is a scarcity of data correlating porosity of metallic bodies with their thermal conductivity, this work was performed to provide such data and to supply samples for use in gas flow testing.

The objectives of the present work were to produce 3/4-inch diameter discs, 1/4, 3/8 and 1/2 inch thick, in high purity copper and 304L stainless steel. The discs were to be made from 105 - 125 micron spherical powder and were to have gross porosities of 10, 20 and 30 percent.

Pure copper was chosen as one test material because of the abundance of thermal data for this metal in its solid form, and stainless steel served as a representative higher strength, high temperature material of lower thermal conductivity.

FABRICATION PROCEDURE

The powders were produced from bar stock by the Rotating Electrode Process.*
This technique utilizes a consumable rotating electrode of the desired alloy,
the end of which is melted by an arc from a non-rotating tungsten electrode
(Figure 1). As the electrode rotates, centrifugal force causes the molten
metal to fly off in the form of fine spherical droplets which freeze in
flight and drop to the floor of the tank. Powder particle size is controlled
by varying electrode diameter and rotational speed. The tank interior is
evacuated and back-filled with helium prior to making powder.

The copper was supplied as 2-1/2-inch diameter OFHC bar, certified to ASTM
B-133. The stainless steel electrode stock was also supplied as 2-1/2-inch
diameter bar; it was certified as AISI 304L. The composition of the electrodes
is given in Table I.

TABLE I. ELECTRODE COMPOSITION (SUPPLIERS'ANALYSES)		
	Copper (%)	304L Stainless Steel (%)
Copper	99.96 min. (including silver)	0.08
Phosphorus	0.0003 max.	0.022
Sulfur	0.0004 max.	0.008
Mercury	0.0010 max.	-----
Zinc	0.0003 max.	-----
Carbon	-----------	0.023
Manganese	-----------	1.68
Silicon	-----------	0.52
Chromium	-----------	18.25
Nickel	-----------	10.10
Molybdenum	-----------	0.06
Iron	-----------	Balance

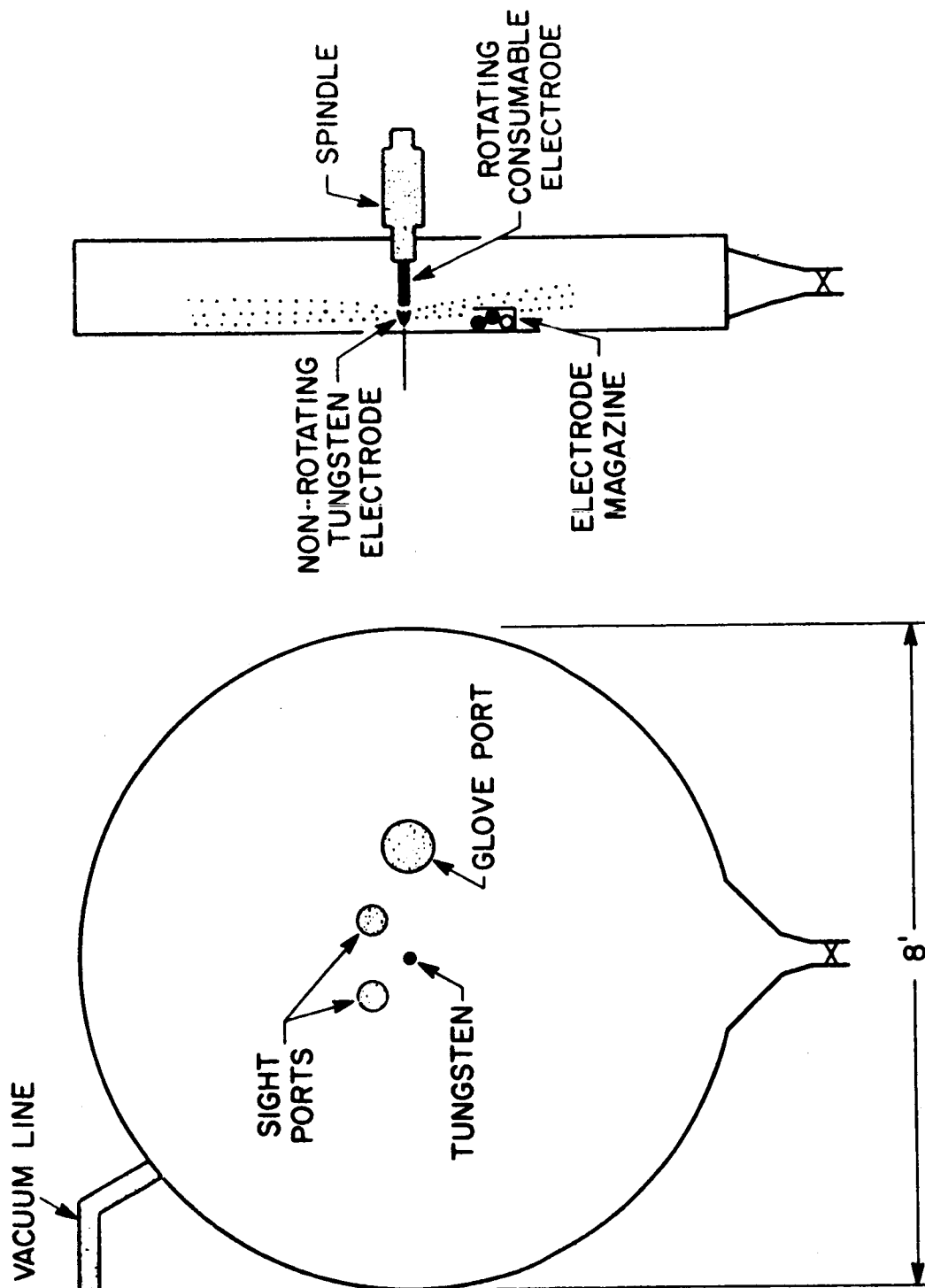* U. S. Patent No. 3,099,041

Figure 1. Rotating electrode unit.

3

The 105 - 125 micron size fraction of each powder was separated from the larger quantity of powder produced. The 105 - 125 micron particles are illustrated in Figure 2. The major-to-minor particle diameter ratio, measured for a random sampling of powders, was 1:1.11 for the copper and 1:1.13 for the stainless steel.

The powders were compacted into porous bars, approximately 1 inch in diameter by 4 inches long, by hot isostatic pressing (10 and 20 percent porosity) and by sintering followed by cold isostatic pressing (30 percent porosity).

Preliminary investigations using 125 - 149 micron powders established that a linear density/temperature relationship (at constant pressure) could be established for the 10 and 20 percent porosity levels for both metals. Further experiments showed that this relationship departs from linearity as the required porosity approaches the 40 percent porosity of the loose powder. It was not feasible to carry out the number of trial runs required to establish the shape of the density/temperature curve in the region of porosities between 20 and 40 percent. The 30 percent porosity samples were therefore prepared by first sintering in dry hydrogen (to clean particle surfaces and to initiate particle bonding) followed by isostatic pressing at room temperature.

The processing parameters for the powder consolidation operation are tabulated in Table II. The procedures for the two types of compaction were:

<u>Hot Isostatic Pressing</u> -- The powders were poured into their respective containers and were fired in hydrogen to clean particle surfaces. Firing conditions were 750°F (400°C) for 1/2 hour for the copper and 2010°F (1100°C) for 1/2 hour for the stainless steel. The containers were evacuated to a pressure of 10^{-5} torr and sealed by electron beam welding. The containers were loaded into the autoclave which was then evacuated and back-filled with argon. The unit was heated until the desired temperatures were reached, at which time the gas pressure was increased to the desired level. Typical heatup times were 2-1/2 hours to reach temperature. At the end of the 2-hour holding period, the gas pressure was relieved and the autoclave cooled to room temperature.

<u>Sinter-Plus-Cold Isostatic-Pressing</u> -- The powders were hydrogen sintered in their compaction containers (copper at 1785°F [975°C] for 1 hour, stainless steel at 2190°F [1200°C] for 1 hour), evacuated and sealed as described above. They were then pressurized at room temperature, in water, in cycles that included approximately 5 minutes to each pressure, 1 minute at pressure and 1 minute to depressurize the autoclave.

After consolidation the containers were machined off, and the disc samples were machined to the required thicknesses of 1/4, 3/8, and 1/2 inch by 3/4 inch in diameter. The thermal conductivity specimens were machined to 1-inch diameter, and the electrical resistivity specimens were machined to 1/4-inch diameter.

4
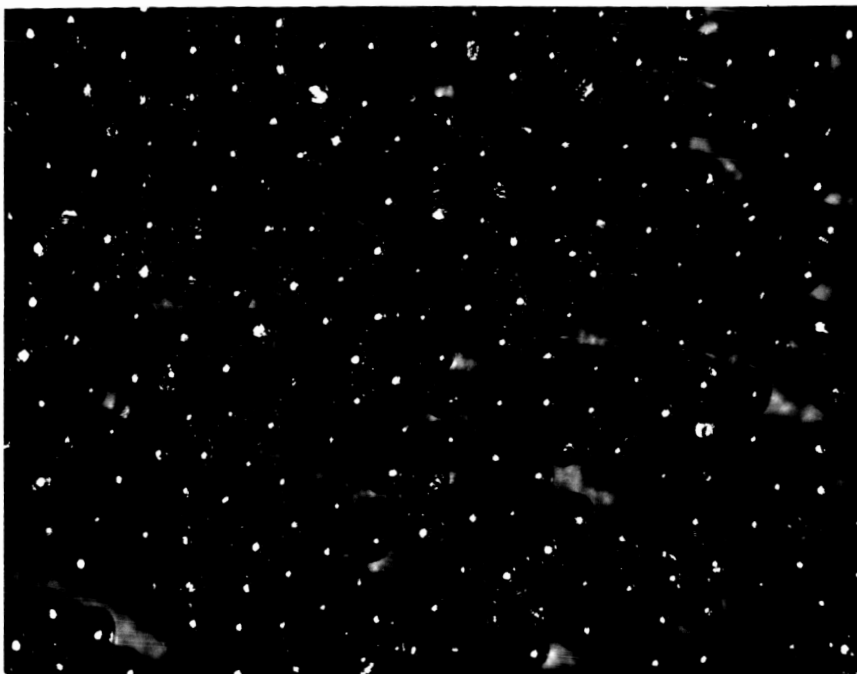
a. Copper

b. Stainless Steel

Figure 2. High purity copper and stainless steel powders, 105 - 125 μ, 50X.

TABLE II. FABRICATION CONDITIONS FOR POROUS COPPER AND STAINLESS STEEL PARTS

Sample Mat'l	Density (% theo.)	Pressing Container Mat'l	O.D. (in.)	Wall (in.)	Length (in.)	Pressure (psi)	Temp. (°C)	Time (hr)	Other
Copper Discs	90	Cu	1.050	.090	5	2550	706	2	Hot isostatic
	80	Cu	1.050	.090	5	2550	595	2	Hot isostatic
	70	Cu	1.050	.090	5	----			5500 psi, cold isostatic
Copper Thermal Conductivity Sample		Cu	1.450	.125	2-1/2				6000 psi cold isostatic
Electrical Resist. Sample		Cu	0.375	.032	2-1/2				6000 psi, cold isostatic
SS Discs	90	SS	1.250	.050	5	2000	1080	2	Hot isostatic
	80	SS	1.250	.050	5	2000	975	2	HIP + 20,000 psi, cold isostatic
	70	SS	1.250	.050	5	----			10,000 psi, cold isostatic
SS Thermal Conductivity Sample		SS	1.500	.060	3				15,000 psi, cold isostatic
SS Electrical Resist. Sample		SS	0.375	.020	2-1/2				15,000 psi, cold isostatic

POWDER TREATMENT PRIOR TO HOT ISOSTATIC PRESSING: Copper -- 400°C, 1/2 hour, in wet H_2
                                                  SS -- 1100°C, 1/2 hour, in dry H_2

POWDER TREATMENT PRIOR TO COLD ISOSTATIC PRESSING: Copper -- 975°C, 1 hour, in wet H_2
                                                   SS -- 1200°C, 1 hour, in dry H_2

Processing conditions had been selected to produce sample densities on the low side of the nominal densities. It was ascertained, after weighing and measuring, that some discs were outside (below) the 2 percent porosity range permitted at each porosity level. These discs were brought into the required density range by encasing them in small polyethylene envelopes placed inside a rubber isostatic pressing bag and pressurizing them at 6,000 to 20,000 psi.

Following their compaction, machining and recompaction (where necessary), the copper discs were stabilized by annealing in hydrogen for 1 hour at 1300°F (706°C). The stainless steel discs, having been processed above the specified 1600°F (871°C) stabilization temperature, did not require such a treatment.

Examination of the machined discs showed that the lathe tool left a smeared surface on each face of the 10 and 20 percent porosity discs. This did not appear to be the case for the 30 percent porosity discs, where the surface particles tore away during the machining operation. The smeared surfaces of the stainless steel discs were removed by electrolytic etching for 10 seconds in a 10 percent aqueous oxalic acid solution at 5 to 15 volts. Smeared surfaces were removed from the copper discs by etching for 10 minutes in an 82.5 percent aqueous orthophosphoric acid solution at 1.0 to 1.6 volts. The etched samples were rinsed in distilled water and methanol and dried at 300°F (190°C). The samples were then reweighed and measured. These data, along with the densities calculated from their thickness, diameters and weights, and their relative densities compared to the rotating electrode reference material, are tabulated in Tables III and IV.

CHARACTERIZATION OF POROUS METAL PARTS

A chemical analysis was performed on each material, using three stainless steel (10 and 20 percent porosity) and three copper (10 and 20 percent porosity) discs to supply enough material for the chemical analyses. The results are shown in Table V. The high phosphorous content shown for the copper represents a surface layer left from the phosphoric acid surface cleaning etch described above. It is believed not to be detrimental to the thermal properties of the copper specimens.

Pores in the compacted parts were characterized by means of visual appearance at a magnification of thirty times; pore size was determined by optical intercept techniques, and by mercury intrusion.

Figures 3 and 4 illustrate typical longitudinal and transverse sections at the interior of 10, 20 and 30 percent porous discs. Examination of three samples in each condition and direction was performed, and the above photographs were selected as representative of the typical homogeneous pore morphology in the samples.

TABLE III. DIMENSIONS AND DENSITIES OF POROUS STAINLESS STEEL DISCS

Sample Number	Nominal Density (%)	Diameter (in.)	Thick. (in.)	Volume (cc)	Weight (g)	Calculated Density (g/cc)	(% of wrought)
Wrought Electrode	100	1.128	.9995	.9990	7.87	7.88	100
1	90	.7475	.2475	1.770	12.44	7.03	89.21
2	90	.7469	.2482	1.781	12.54	7.03	89.21
3	90	.7475	.2500	1.798	12.67	7.04	89.33
4	90	.7463	.3712	2.661	18.80	7.06	89.59
5	90	.7476	.3726	2.680	19.09	7.12	90.35
6	90	.7480	.3732	2.687	19.01	7.07	89.72
7	90	.7472	.3737	2.685	19.04	7.09	89.97
8	90	.7481	.4995	3.598	25.56	7.10	90.10
9	90	.7493	.4992	3.607	25.60	7.09	89.97
10	90	.7479	.4996	3.598	25.51	7.09	89.97
11	80	.7485	.2475	1.785	11.14	6.24	79.19
12	80	.7524	.2494	1.817	11.18	6.15	78.04
13	80	.7460	.2455	1.759	11.04	6.27	79.57
14	80	.7445	.3695	2.635	16.24	6.16	78.17
15	80	.7460	.3695	2.647	16.47	6.22	78.93
16	80	.7445	.3690	2.632	16.29	6.18	78.42
17	80	.7465	.3690	2.647	16.23	6.13	77.79
18	80	.7450	.4940	3.528	21.72	6.15	78.04
19	80	.7516	.4982	3.573	22.27	6.23	79.06
20	80	.7470	.4960	3.563	22.34	6.26	79.44
21	70	.7360	.2475	1.725	9.40	5.45	69.16
22	70	.7475	.2476	1.771	9.54	5.38	68.27
23	70	.7510	.2516	1.827	9.66	5.28	67.00
24	70	.7501	.3738	2.707	14.67	5.41	68.65
25	70	.7481	.3754	2.704	14.53	5.37	68.14
26	70	.7493	.3744	2.706	14.66	5.41	68.65
27	70	.7484	.3762	2.712	14.55	5.36	68.02
28	70	.7521	.5023	3.656	19.57	5.35	67.89
29	70	.7491	.4992	3.606	19.43	5.38	68.27
30	70	.7490	.5000	3.611	19.42	5.37	68.14

Sample Number	Nominal Density (%)	Diameter (in.)	Thick. (in.)	Volume (cc)	Weight (g)	Calculated Density (g/cc)	(% of wrought)
TABLE IV. DIMENSIONS AND DENSITIES OF POROUS COPPER DISCS							
Wrought Electrode	100	1.126	.9993	.995	8.87	8.91	100.00
31	90	.7480	.2450	1.763	13.98	7.93	88.97
32	90	.7500	.2470	1.787	14.18	7.94	89.09
33	90	.7500	.2500	1.810	14.46	7.99	89.65
34	90	.7500	.3730	2.699	21.48	7.96	89.31
35	90	.7500	.3700	2.679	21.36	7.97	89.42
36	90	.7500	.3720	2.693	21.37	7.93	88.97
37	90	.7495	.3774	2.729	21.75	7.97	89.42
38	90	.7500	.4980	3.605	28.72	7.97	89.42
39	90	.7500	.4980	3.605	28.76	7.98	89.53
40	90	.7500	.4960	3.591	28.63	7.97	89.42
41	80	.7440	.2500	1.781	12.51	7.02	78.76
42	80	.7460	.2500	1.791	12.74	7.11	79.77
43	80	.7470	.2480	1.782	12.53	7.03	78.88
44	80	.7520	.3730	2.713	19.01	7.01	78.65
45	80	.7520	.3700	2.693	19.03	7.07	79.32
46	80	.7520	.3710	2.699	19.00	7.04	78.99
47	80	.7520	.3768	2.742	19.51	7.11	79.77
48	80	.7520	.4970	3.616	25.33	7.00	78.54
49	80	.7480	.4930	3.549	25.34	7.14	80.11
50	80	.7480	.4990	3.592	25.46	7.09	79.55
51	70	.7465	.2465	1.768	10.98	6.21	69.68
52	70	.7510	.2485	1.803	11.21	6.22	69.79
53	70	.7510	.2485	1.803	11.20	6.21	69.68
54	70	.7520	.3730	2.713	17.08	6.30	70.69
55	70	.7465	.3705	2.657	16.65	6.27	70.35
56	70	.7467	.3693	2.650	16.31	6.15	69.00
57	70	.7520	.3750	2.730	17.18	6.29	70.57
58	70	.7375	.5040	3.528	22.28	6.40	71.81
59	70	.7270	.4970	3.380	21.17	6.26	70.24
60	70	.7390	.4970	3.492	22.18	6.35	71.25

TABLE V. CHEMICAL ANAYLSES OF POROUS DISCS		
	Copper (80% dense)	Stainless Steel (90% dense)
Cadmium	< 0.5 ppm	-------
Phosphorus	200	-------
Sulfur	5	-------
Zinc	1	-------
Mercury	< 1	-------
Lead	5	-------
Selenium	< 2	-------
Tellurium	2	-------
Bismuth	< 0.5	-------
Arsenic Antimony Bismuth Selenium Tellurium Tin Manganese	<14	-------
Chromium	------	18.15%
Nickel	------	10.09
Manganese	------	1.87
Silicon	------	0.58
Carbon	------	0.030
Oxygen	520	0.031

Longitudinal   Porosity   Transverse
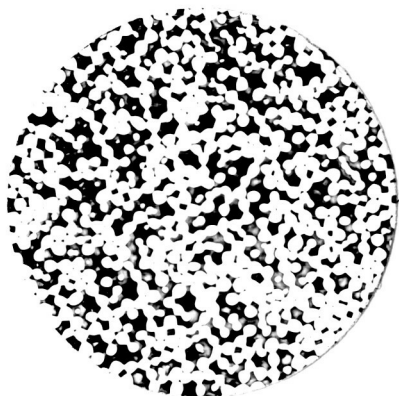
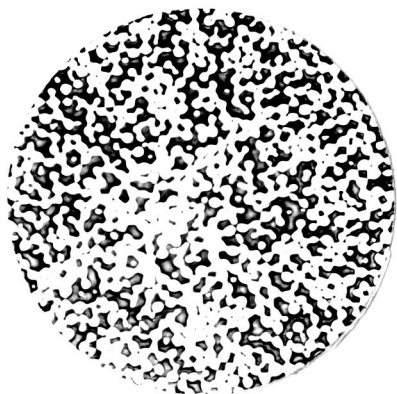SS 70-1,L   Plate 297   30%   SS 70-1,T   Plate 297A
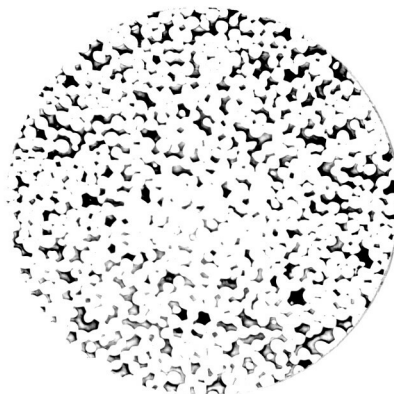
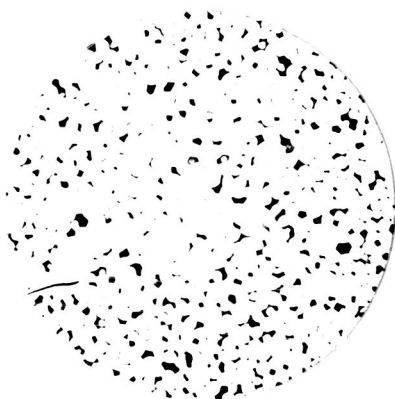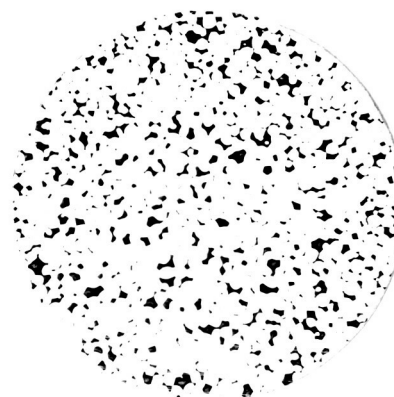SS 80-1,L   Plate 297F   20%   SS 80-1,T   Plate 297G
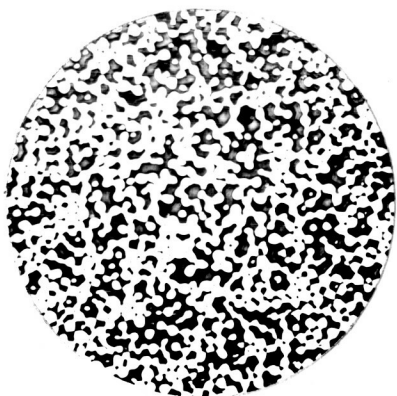
SS 90-1,L   Plate 297L   10%   SS 90-1,T   Plate 297M

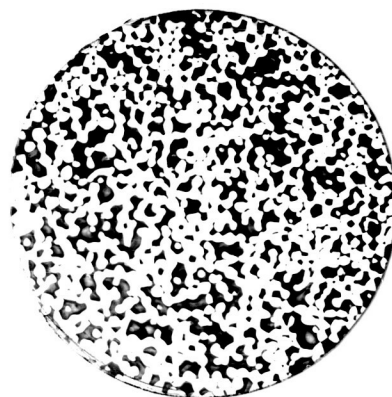Figure 3.   Porous stainless steel parts, 15X.

Longitudinal	Porosity	Transverse

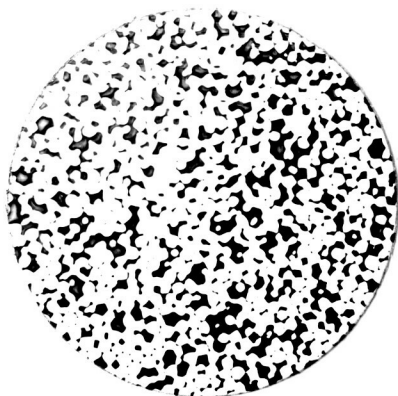Cu 70-3,L   Plate 295B   30%   Cu 70-2,T   Plate 295A$_2$

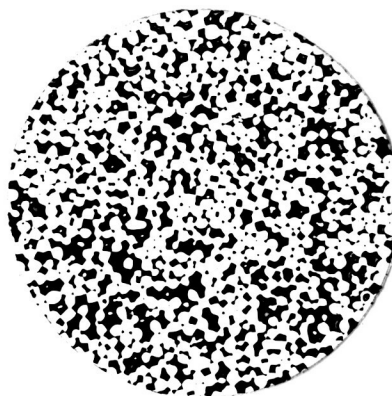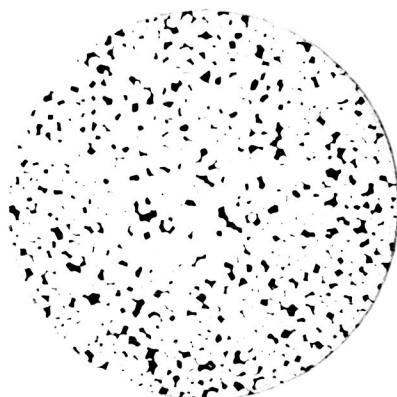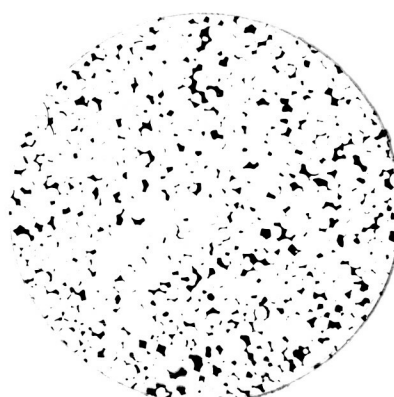Cu 80-1,L   Plate 295C$_1$ 20%   Cu 80-3,T   Plate 295E$_2$

Cu 90-2,L   Plate 295G$_1$ 10%   Cu 90-2,T   Plate 295G$_2$

Figure 4. Porous copper parts, 15X.

Mercury intrusion is a technique for measuring the diameter of pores or pore channels that interconnect to the surface of the specimen, i.e., are "open" pores. The measuring technique is based upon the relationship that exists between the pore or channel diameter, d, and a pressurizing fluid which intrudes into the open pores. In general form this relationship is:

$$d = \frac{4\gamma(\cos \phi)}{\rho}$$

where γ = surface tension of the intruding fluid

              ϕ = wetting angle between the fluid and material under test

              ρ = fluid pressure

Using mercury as the intruding fluid, the relationship reduces to:

$$d = \frac{175}{\rho}$$

with d in microns when pressure is expressed as pounds per square inch. (For this relationship to be valid, it is essential that the test material not be wetted by the intruding fluid. The copper samples were therefore oxidized in air for five minutes at 750°F (400°C).

The intrusion measurements are performed as follows: By placing a test sample in a chamber which is first evacuated and then filled with mercury, one can measure the drop in mercury level in the precisely calibrated test chamber with increasing pressurization. The volume of pores intruded at each pressure level can therefore be calculated, and by use of the relationship noted above, the intruded volume can be related to the pore size.

Figures 5 through 10 illustrate the pore size spectra for the 10, 20 and 30 percent porosity stainless steel and copper materials. The bi-modal form of the copper spectra at the small-pore end of the scale is due to a breakdown of the oxide film in the small-pore/high-pressure region of intrusion. The film breakdown gives the appearance of a large percentage of small pores as mercury combines with the copper metal. The mercury porisimeter merely records the drop in mercury level at each pressure level and cannot differentiate between mercury "lost" in small pores and mercury "lost" by amalgamation. Since the breakdown occurs in a region of very small pores in low concentration, it is considered to have only a minor effect on the calculation of mean pore size.

Figure 5. 304 stainless steel, 105 - 125 micron, 30 percent nominal porosity.
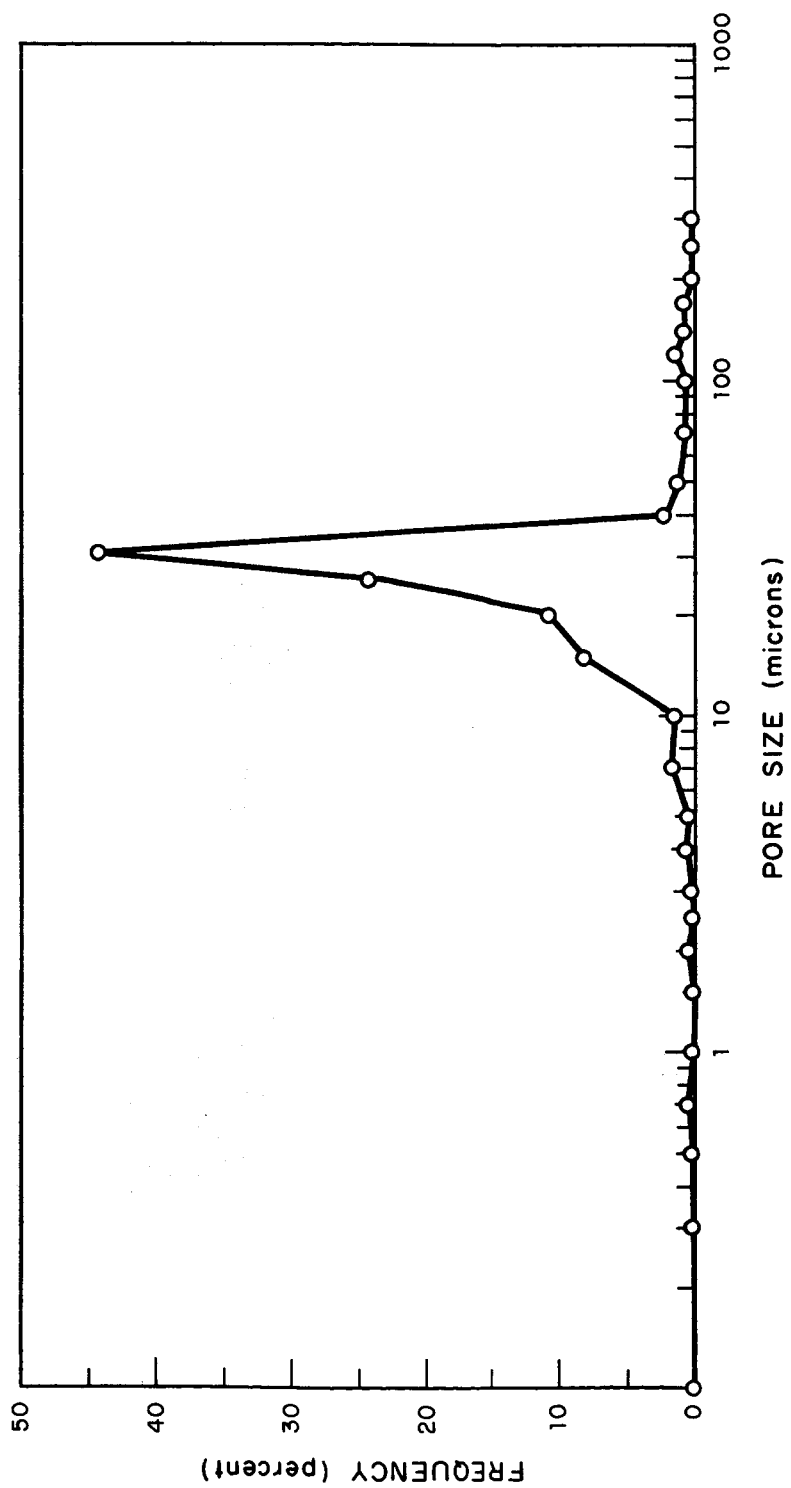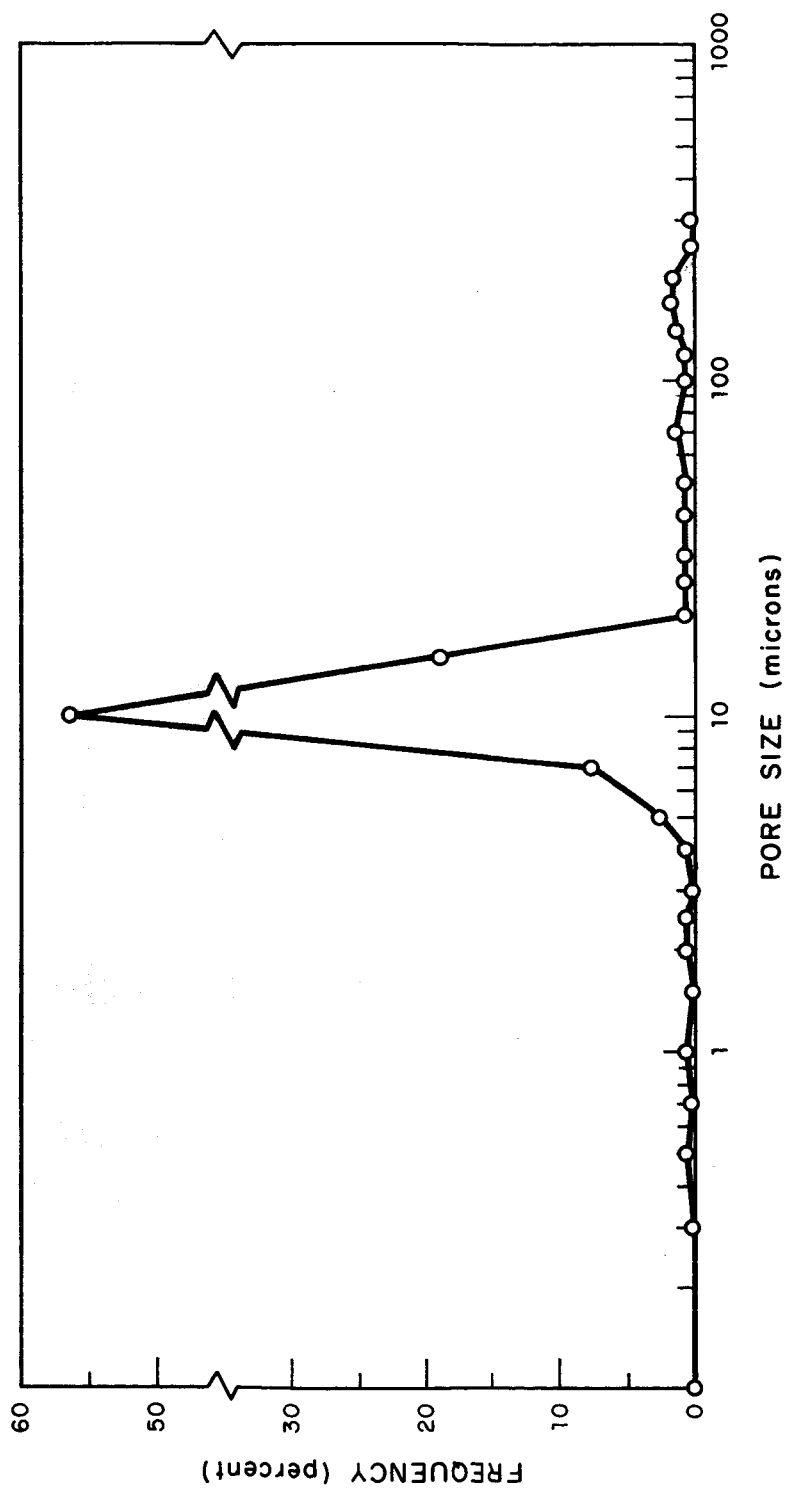
Figure 6. 304 stainless steel, 105 - 125 micron, 20 percent nominal porosity.
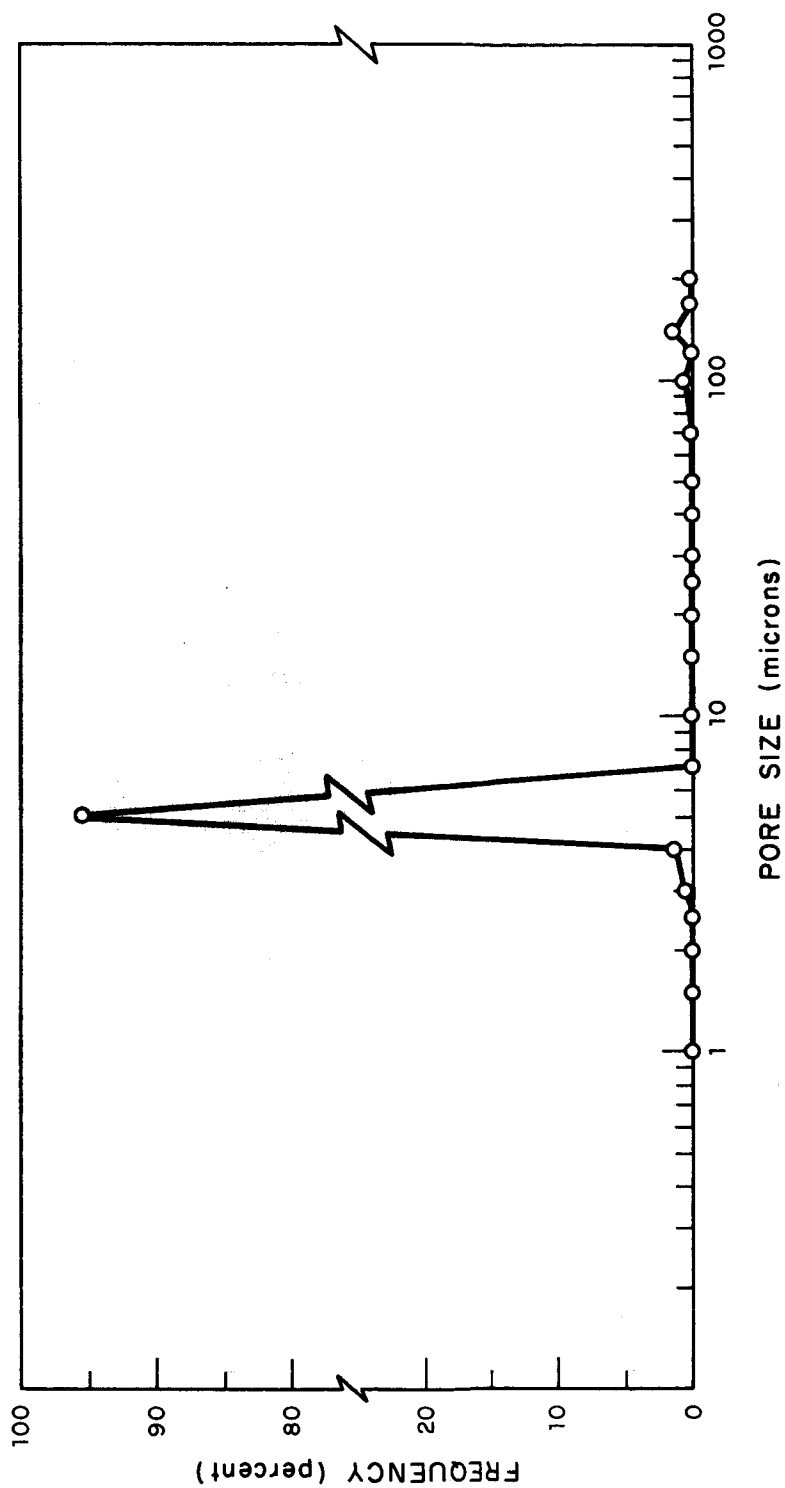
Figure 7. 304 stainless steel, 105 – 125 micron, 10 percent nominal porosity.
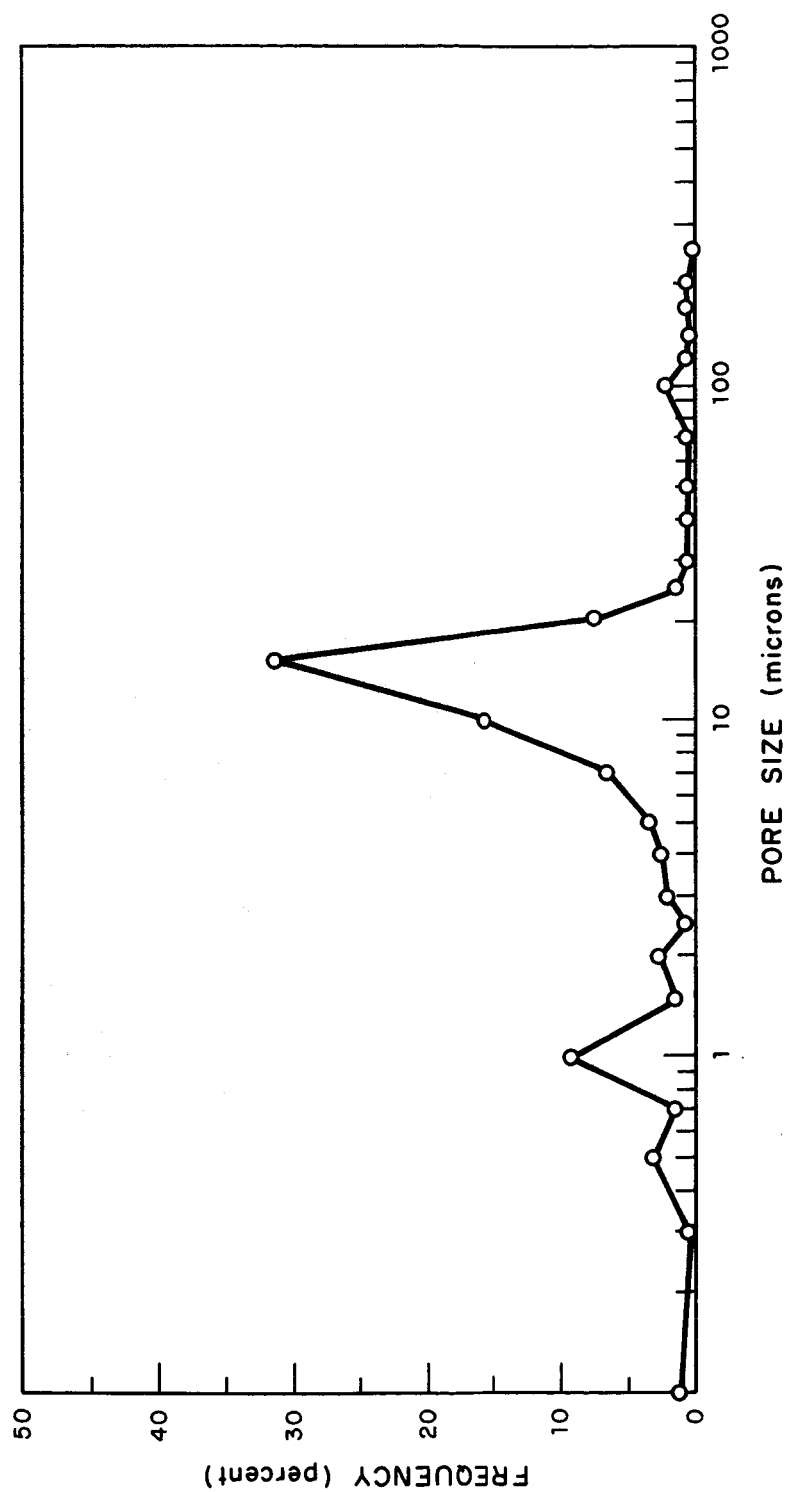
16

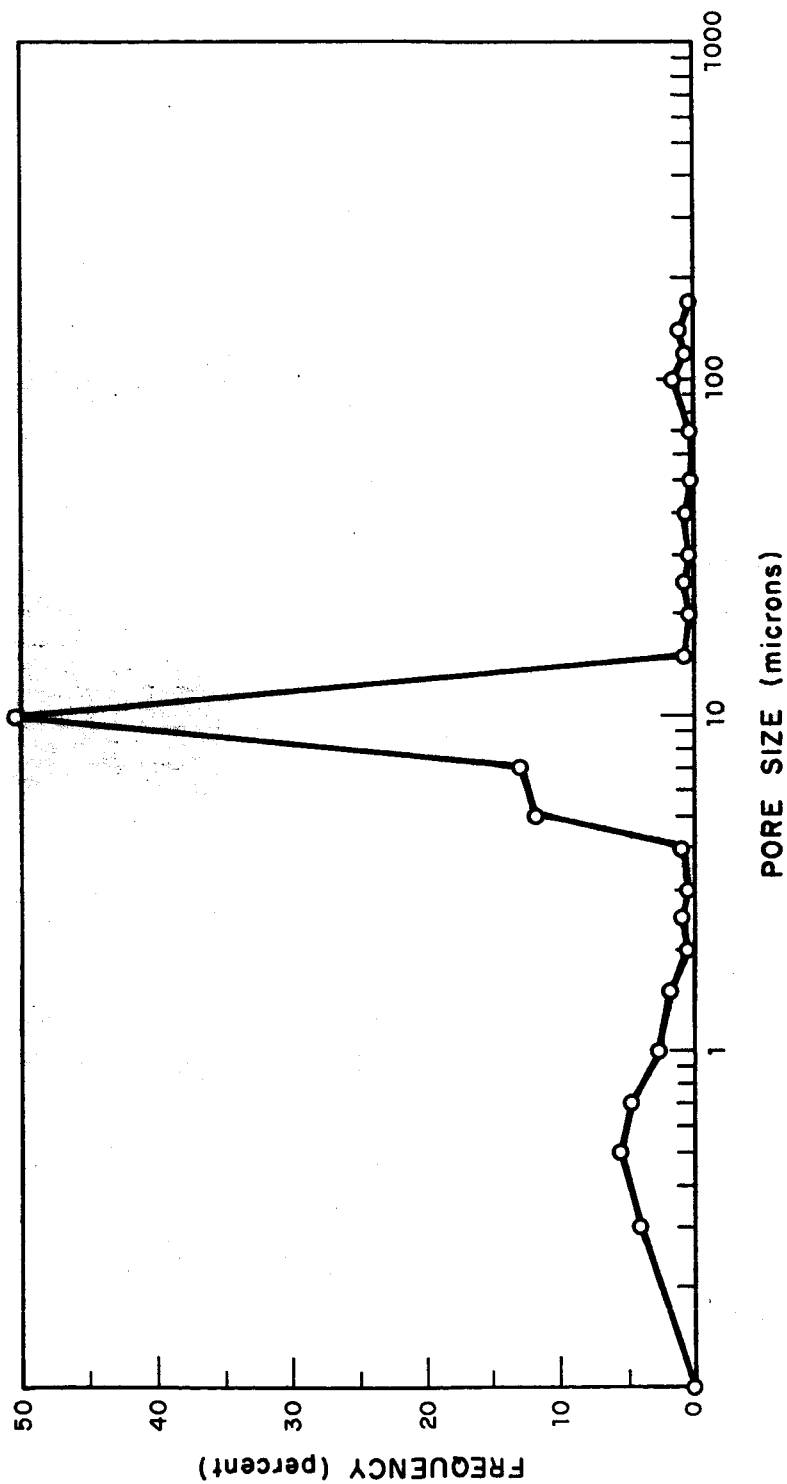Figure 8. OFHC copper, 105 - 125 micron, 30 percent nominal porosity.

17

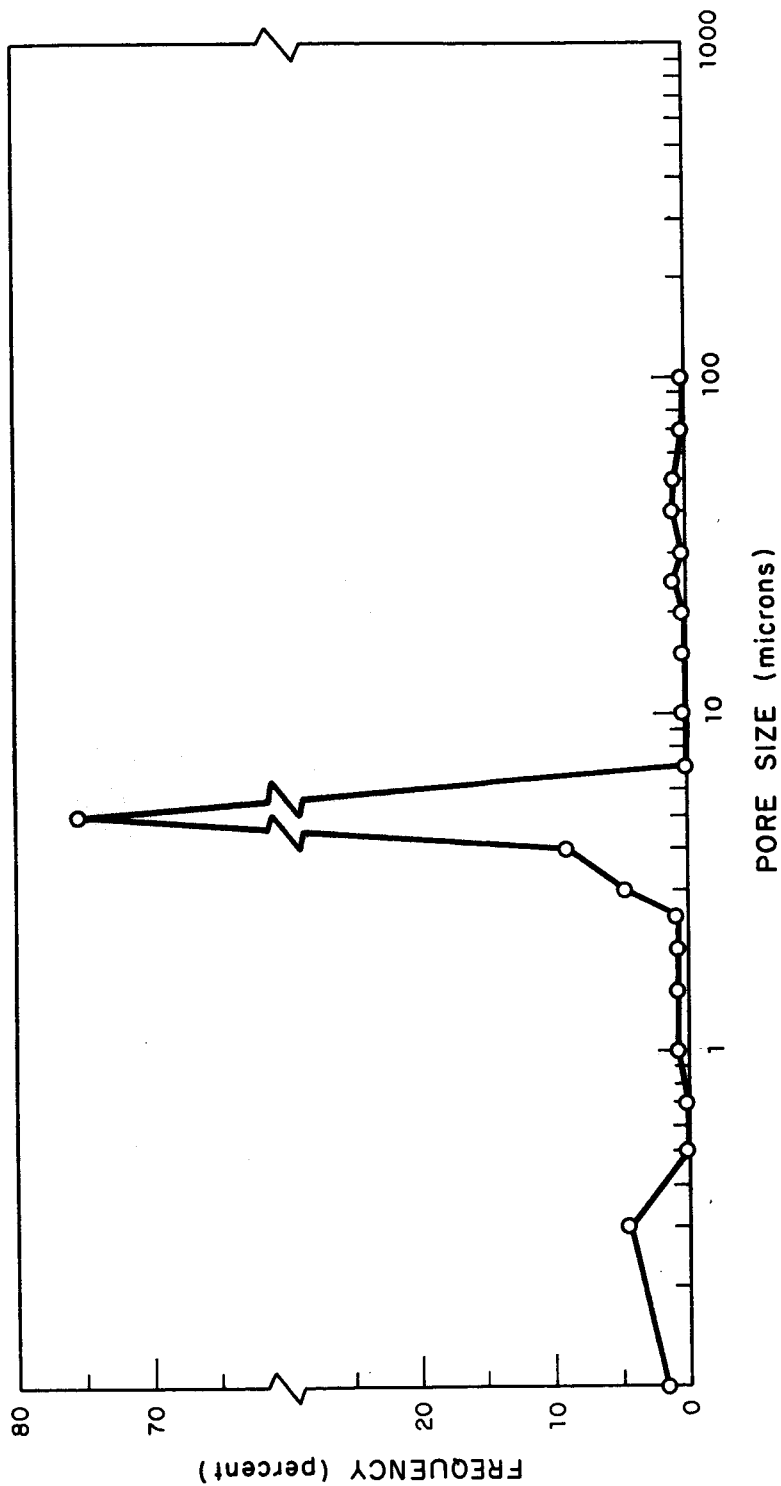Figure 9. OFHC copper, 105 - 125 micron, 20 percent nominal porosity.

Figure 10. OFHC copper, 105 - 125 micron, 10 percent nominal porosity.

19

The mean pore size was obtained by integrating the incremental intruded pore volumes for each sample. The intruded pore volumes, i.e., the total void space occupied by the mercury, are presented on a unit basis as cubic centimeters void per gram of specimen. Mean pore size and total intruded pore volume are tabulated in Table VI.

TABLE VI. MERCURY INTRUSION OPEN PORE VOLUME AND MEAN PORE SIZE
FOR POROUS STAINLESS STEEL AND COPPER PARTS

Nominal Porosity (%)	Total Intruded Open Pore Volume (cc/g)	Mean Pore Size (microns)
STAINLESS STEEL		
10	0.0135	7.67
20	0.0242	21.2
30	0.0479	29.6
COPPER		
10	0.0113	5.30
20	0.0225	10.1
30	0.0383	16.6

Pore size and pore volume were also measured by optical techniques. The technique used is based on that described by Smith and Guttman.* Photographs, at a magnification of 150 times, were taken of random areas of copper and stainless steel samples, in both longitudinal and transverse directions. A grid was applied to each photograph, and measurements were made of the number and length of pore intercepts. (Figure 11 illustrates a typical sample photograph with the superimposed grid lines.) The porosity in each sample was then obtained by the relationship

$$\text{Porosity (pore fraction), } \epsilon, = \frac{L_a}{L}$$

* C. S. Smith and L. Guttman, "Measurement of Internal Boundaries in Three-Dimensional Structures by Random Sectioning," Transactions of the AIME, Journal of Metals, January 1953, pp. 85-87.
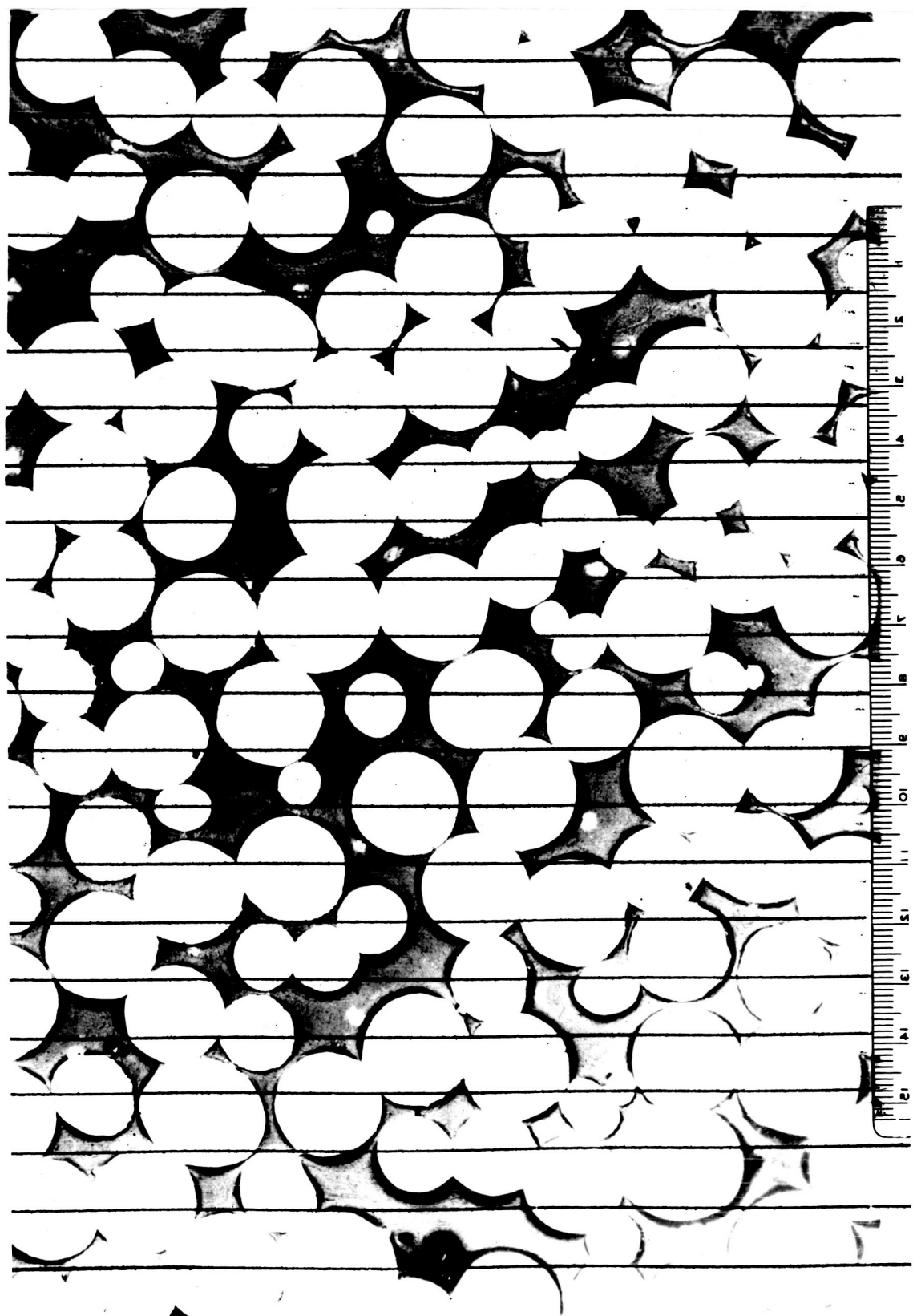
Figure 11. Pore size and pore volume measurements.

where L_a = total length of line traversing pores

L = total length of grid line in area of measurement.

The surface area of the pores was measured by a second relationship

$$\text{Volume to surface area ratio, } \beta = \frac{2N}{L}$$

where N = number of intercepts of the grid lines with pores in the area of measurement.

With the information so obtained, it was possible to calculate the hydraulic pore diameter (HPD) for the samples, using the relationship

$$\mu = \text{HPD} = \frac{2\epsilon}{\beta}$$

Table VII lists the values obtained for ϵ and μ . Examination of the table shows internal contradictions: e.g., values for μ for stainless steel at 30 percent and 20 percent porosity, longitudinal; and for copper at 30 percent and 20 percent porosity, transverse direction. There are also discrepancies between optical values and values obtained by bulk measurements and by mercury intrusion, such as pore fraction and pore size. These discrepancies are attributed to the size of our sampling "population" and would most likely disappear if the number of data points had been increased by using lower magnification photographs (more particles under grid) and the size of the grid spacing had been decreased.

CONDUCTIVITY*

Thermal and electrical conductivity were determined for both the stainless steel and copper at each porosity. The tests were performed on 1-inch (thermal conductivity) and 1/4-inch (electrical conductivity) cylindrical samples machined from special bars compacted at the same time as the

---

* All thermal and electrical measurements were carried out by Dynatech Corporation, Cambridge, Massachusetts, under subcontract to Whittaker Corporation

Nominal Porosity (%)	L_a* (microns) Long./Trans.		L* (microns)	Pore Fraction* Long./Trans.		N* Long./Trans.		HPD* (microns) Long./Trans.	
			STAINLESS STEEL						
30	6630	6750	4368mm	.228	.232	336	353	19.7	19.1
20	6710	2555	or	.230	.0877	361	252	18.6	10.1
10	2808	2735	29,134μ	.0964	.0939	289	249	9.72	11.0
			COPPER						
30	8317	3762	4368mm	.285	.129	401	308	20.7	12.2
20	6863	5790	or	.235	.199	366	378	18.8	15.3
10	3282	2068	29,134μ	.113	.071	260	222	12.6	9.32

TABLE VII. PORE DESCRIPTION BY OPTICAL MEANS

* L_a = total length of intercepts

    L = total length of grid line

    Pore Fraction, ϵ, = $\dfrac{L_a}{L}$

    N = number of intercepts

    HPD,= μ, $\dfrac{L_a}{N}$

respective stainless steel and copper disc sample bars. Specimens machined from the wrought powder-making electrode produced reference (100 percent density) values. The thermal and electrical conductivity data for tests run in vacuum at temperatures to 1290°F (700°C) for copper and 1650°F (900°C) for stainless steel are contained in the appendix.

CONCLUSIONS

The ability to manufacture uniform 10, 20 and 30 percent porosity stainless
steel and copper parts from high purity closely sized powders was demon-
strated by producing thirty copper and thirty stainless steel discs, 3/4 inch
in diameter by 1/4, 3/8 and 1/2 inch in thickness. Uniformity of porosity
within the parts and from part to part was demonstrated by bulk measurements
of weight and dimensions, by mercury intrusion and by optical techniques.

DYNATECH

AN EXPERIMENTAL INVESTIGATION OF THE THERMAL CONDUCTIVITY
AND ELECTRICAL RESISTIVITY OF POROUS COPPER AND
304L STAINLESS STEEL MATERIALS MANUFACTURED
BY POWDER METALLURGY METHODS

By

R. P. Tye

Report WHT-1

This report covers work carried out on behalf of:

Whittaker Corporation
Nuclear Metals Division
West Concord, Massachusetts 01781

P.O. #68-07858

This work was performed in support of NASA Contract NAS 3-13309
Lewis Research Center and Monitored by Mr. G. Friedmann of
Nuclear Metals and Mr. A. Fortini of NASA

Progress through Research

DYNATECH

AN EXPERIMENTAL INVESTIGATION OF THE THERMAL CONDUCTIVITY AND ELECTRICAL RESISTIVITY OF POROUS COPPER AND 304L STAINLESS STEEL MATERIALS MANUFACTURED BY POWDER METALLURGY METHODS

A. Introduction

The comparative cut bar method of measuring thermal conductivity with samples approximately 25 mm diameter and long has been used to evaluate the conductance in vacuum of three different porosities of a pure copper and a 304 L stainless steel manufactured from sintered spherical powder particles. In addition the dense base materials were evaluated over the same approximate temperature range of 300 to 1200K.

Electrical resistivity determinations were made on small rod shaped samples of materials of closely similar porosity to the thermal conductivity samples over the above temperature range.

B. Object of the Investigation

Porous metals are of importance in transpirational cooling problems over a wide temperature range. For design purposes, basic property data are required for the newer types of materials now being used particularly at temperatures up to 1300K and for different environments.

The total thermal conductivity λ_T of such a material may be represented by

$$\lambda_T = \lambda_E + \lambda_R + \lambda_{C_1} + \lambda_{C_2} \tag{1}$$

where λ_E is the component due to electronic conduction λ_e plus lattice conduction λ_g, λ_R is the component due to radiation, λ_{C_1} is the component due to gas within the trapped pores including any possible convection and λ_{C_2} is the component due to gas

Progress through Research

DYNATECH

within the open pores including any possible convection. In vacuum, this λ_{C2} is zero. For materials of low porosity λ_{C_1} will be very small so that the total quantity measured will normally be due to the λ_E and λ_R contributions only.

For electrical conductors the Lorenz number L is given by

$$L = \frac{\lambda_E \rho}{T} \qquad (2)$$

$$\lambda_E = \lambda_e = \lambda_g \qquad (3)$$

$$\lambda_e = \frac{L_o T}{\rho} \qquad (4)$$

Here λ is in the $W\ m^{-1}\ deg^{-1}$ unit, ρ in the ohm m unit, T the absolute temperature, K and L will thus be in the $V^2\ deg\ K^{-2}$ unit. For eq (4) L_o is the usual Sommerfeld theoretical value of the Lorenz number ($2.443 \times 10^{-8}\ V^2\ deg\ K^{-2}$).

Electrical resistivity is a function of electronic conduction only. Thus measurements of ρ and λ_E in vacuum coupled with the assumption that λ_e can be calculated from (3) can lead to the separation of the different components. Measurements will lead not only to true effective properties at elevated temperatures but also to possible examination of the behaviour of the different components with temperature.

In most cases λ_g varies as T^{-1}. At temperatures well in excess of the Debye temperature, for a particular system, λ_e is the predominant transport mechanism. However, it has been found empirically from measurements in the range 200 to 800K on different alloy systems that the Wiedermann-Franz-Lorenz relationship may be modified in the following manner

$$\lambda_E = \frac{L_1 T}{\rho} + b, \qquad (5)$$

where L_1 is a number similar to the Sommerfeld value, b is a constant lattice component. This form of relationship has proved very useful in the prediction of the thermal conductivity behaviour of new alloys of particular systems from the relatively simple measurement of electrical resistivity. This has proved true for some porous

DYNATECH

metal systems in addition. It is, therefore, a possibility that some form of empirical relationship may hold for the particular type of porous metal now studied.

The materials investigated were manufactured from spherical powder particles obtained from oxygen free high conductivity copper and 304L stainless steel stock respectively. Pieces of the original stock of each metal were retained and samples prepared from them in order to provide base points for the nominal 100% dense materials.

C. Materials Studied

Two samples of each material were supplied

1. A thermal conductivity sample approximately 25 mm diameter and 25 mm long with two small holes approximately 1.3 mm diameter drilled across the sample at levels approximately 3 mm from each surface. The surfaces of the sample were prepared as flat and smooth as possible in order to make sure that the total thickness was uniform and the faces were parallel.

2. An electrical resistivity sample 6 mm diameter and 30 to 40 mm long, with two small radial holes 0.3 mm diameter drilled 3 mm deep located on the central line.

On receipt, all dimensions were measured accurately. Following this, electrical resistivity measurements were made at room temperature as follows.

For the purposes of the test the ends of the sample were fitted with current electrodes and then laid on knife edges a fixed distance apart. A steady d.c. current from a 24 V battery was applied to the sample and the potential drop developed across the knife edges was measured with a Leeds & Northrup potentiometer in addition to that developed across a calibrated 0.001 Ω resistance in series with the sample. The current was reversed to eliminate thermal voltages and the potential measurements repeated. The electrical resistivity was derived in terms of the ratio of the above voltages the gross cross sectional area and the separation of the knife edges.

Details of the samples supplied are given in Table I.

DYNATECH

D. Test Procedures

(a) Thermal Conductivity: for the purpose of the test, fine gauge (0.2 mm diameter) platinum 10% rhodium/platinum thermocouples insulated in twin bore alumina 1.3 mm diameter tubing were fixed tightly into the holes and discharged welded at a position close to the centre of the sample so that the thermocouple bead was in good contact with the metal. A small piece of alumina tubing was inserted in the opposite end of the hole. The sample was placed between two similar sized samples of a reference material of known thermal conductivity for the range covered. For the stainless steel materials, Inconel 702,[1,2] a complex nickel chromium alloy, was used. For the coppers, Armco iron[3] was used for the highest porosity, and a pure copper[4] for the other three samples. To help reduce contact resistance a thin layer (0.05 mm) of palladium foil was placed between the contacting surfaces. A reproducible load of approximately 10^6 N m^{-2} was applied to the top of the sample stack to assist in reducing contact resistances. A 75 mm diameter alumina guard tube which could be heated independently over a number of sections along its length and which contained thermocouples fixed at positions opposite the thermocouples and joints in the sample stack was placed around the stack and the interspace and surrounds packed with dry sil-o-cel thermal insulating powder which had been degassed at 450C for a period of time. The complete assembly was covered with a bell jar and the enclosure was evacuated to a pressure lower than 10^{-3} torr. Figure I shows a schematic assembly of the Dynatech TCCGM thermal conductivity apparatus used.

By means of suitable adjustments to the power in the various heaters and of the cold sink temperature, a steady temperature distribution was maintained in the system. Undue radial loss was prevented by keeping the guard tube gradient matched to that along the combined sample stack by adjustment of the individual heaters in the guard tube.

Equilibrium conditions were attained normally in the order of 6 to 8 hours after any large adjustment of power to attain a set temperature level. During this period of time small adjustments were made to the individual guard tube heaters to ensure

Progress through Research

DYNATECH

that the guarding was as good as possible.

At equilibrium conditions the temperature at various points in the system were evaluated from the thermocouple readings obtained with the potentiometer. The heat flow Q, in the test specimen was derived in terms of that flowing through each reference material from

$$Q = \lambda_r \ A \ \frac{dT}{dx} \tag{6}$$

where A is the area of cross section, dx the distance between the thermocouple positions in the appropriate reference material, dT the respective temperature difference and λ_r the thermal conductivity of the reference material at its appropriate mean temperature.

The thermal conductivity of the test sample was evaluated from a knowledge of the mean heat flow in the upper and lower reference materials, the temperature difference across the sample and its known dimensions.

Measurements were made in the above manner at successive increasing mean temperatures in the approximate range 300 to 1200K and a repeat measurement taken at a lower temperature in that range after attaining the highest temperature.

Table II contains the following details of the evaluation of thermal conductivity in this investigation:

1. A copy of a complete set of data and the subsequent evaluation of λ for a random data point for each material.

2. A table listing the individual data points, showing the spread between the individual heat flows in the reference materials.

(b) Electrical Resistivity: two thermocouples were fixed tightly into small holes drilled approximately 20 mm apart on the central section of each rod.

DYNATECH

Current leads were attached to each end and the sample assembled at the centre of a furnace which could be heated uniformly. Measurements were made as described previously in Section C except that now the potential difference across the sample was measured using the "like" arms of the two thermocouples at successive increments of temperature in a protective gas environment over the temperature range covered in the thermal conductivity measurements. Repeat measurements were taken on cooling in all cases, in order to see if any changes had been produced by the heat treatment.

E. Results

The experimental results of the thermal conductivity are given in Figures 2a and b for the copper and stainless steel materials respectively. Those for electrical resistivity are shown in Figures 3a and b respectively, Tables III and IV contain values at regular increments of temperature obtained from smooth curves drawn through the experimental points together with those for the derived Lorenz number, L, for the copper and stainless steel respectively.

The results obtained for the two solid materials agree very well with those obtained elsewhere and which are given in the collected data published by the Thermophysical Properties Research Center of the University of Purdue and for the case of copper are summarized in NSRDS-NBS 8. This factor would indicate the methods chosen are capable of providing reliable results for the respective properties. However, it might be pointed out that the comparative cut bar method was used for the copper materials only because of the limitations imposed by the availability of the material. It would have been preferable to use a long thin rod sample where the length to diameter ratio was at least 8 to 1. While every effort was made to undertake the measurements on these copper materials with the highest accuracy possible, it can be seen that the temperature drops across the respective pieces of the sample stack were rather small. Despite this and the fact that the measurements were carried out in vacuum, which would tend to produce uncertainties in contact resistances, it would appear that the consistent results were obtained and there were only small temperature drops at the interfaces. It is estimated that the accuracy of measurement is within ±5% for the stainless steel materials and ±8% for the coppers.

Progress through Research

DYNATECH

For both materials there is a considerable decrease in thermal conductivity accompanied by an increase of electrical resistivity as the porosity of the materials increases. Significantly, however, the Lorenz numbers at the respective temperatures are close to those for the solid material at the same temperature to well within 10%. Furthermore, the Lorenz numbers for the present stainless steel material are in good agreement with those obtained previously for the Rigimesh stainless steels (See NASA CR 72710). It would seem therefore that for future materials of these systems the thermal conductivity can be derived from the use of a mean value of L at a respective temperature or one from a modified Wiedemann Franz relationship obtained from those results together with approximate electrical resistivity values.

F. <u>References</u>

1. H. E. Robinson and D. R. Flynn, "The Current Status of Thermal Conductivity Reference Standards at the National Bureau of Standards," The Third Conference on Thermal Conductivity, Vol. I (1963).

2. M. J. Laubitz, "Inconel 702 – Thermal Conductivity Standard," The Third Conference on Thermal Conductivity, Vol. I, (1963).

3. R. W. Powell, "NPL Work on Thermal Conductivity Standards," The Third Conference on Thermal Conductivity, Vol. I (1963).

4. "Thermal Conductivity of Selected Materials," NSRDS-NBS 8 (1966).

TABLE I

Details of Samples Supplied for the Investigation

Material	Stated Porosity, %	Dimensions, mm	Distance between holes, mm	Electrical Resistivity at 24C, $10^8 \Omega$ m
Copper	0	25.4 d, 25.4 l	19.1	–
	10.31	25.1 d, 25.4 l	19.0	–
	20.96	25.4 d, 25.4 l	19.0	–
	30.09	25.5 d, 25.4 l	18.9	–
	0	6.35 d, 31.1 l	15.5	1.794
	10.31	6.35 d, 45.2 l	20.0	2.28
	20.96	5.73 d, 40.1 l	13.9	3.49
	30.77	6.27 d, 38.9 l	14.5	4.76
Stainless Steel	0	25.5 d, 25.4 l	19.2	–
	9.2	25.6 d, 25.3 l	19.0	–
	21.38	25.6 d, 25.4 l	19.0	–
	31.0	25.4 d, 25.2 l	19.0	–
	0	6.45 d, 31.5 l	17.1	72.1
	9.28	6.39 d, 42.4 l	26.0	95.2
	21.58	6.40 d, 26.6 l	15.1	135.3
	31.99	6.30 d, 40.1 l	20.7	230.5

TABLE IIa

Details of Conditions for Each Data Point for Copper Materials

Sample	Temperature C							Heat Flow Difference, %* T-B
	Top Heat Meter, T		Sample		Bottom Heat Meter, B		λ_T Measured	
	Mean	ΔT	Mean	ΔT	Mean	ΔT		
0 porosity	+	+	129	6.6	+	+	393.5	2.7
	+	+	271	8.2	+	+	381	-5.1
	+	+	382	8.8	+	+	374.5	-3.7
	515.5	9.2	501	9.7	489.9	9.5	357.5	-4.0
	694.8	9.2	681	9.3	579.2	9.05	345.5	5.3
	205.5	6.4	195	6.5	186.4	6.7	390.5	-5.8
9.63 porosity	+	+	141	8.0	+	+	317.5	-6.6
	+	+	387.5	9.6	+	+	298	3.2
	622.7	6.7	611	8.5	599.8	6.25	276.5	7.1
	730.5	7.55	718	10.1	708.0	7.6	269	-0.7
	+	+	229	7.7	+	+	308	-5.8
19.99 porosity	139.8	5.05	129.5	8.6	119.3	5.1	226	3.8
	378.3	4.7	367	9.2	356.5	4.9	198	-4.6
	553.5	4.5	544	9.0	536.0	4.35	181	2.3
	+	+	659	8.5	+	+	163	-1.7
	+	+	167	15.4	+	+	227	-12.8
	333.0	4.7	324	8.8	315.1	4.75	207	-5.2
30.09 porosity	155.8	26.7	131	10.5	106.7	25.9	163	-2.6
	292.2	34.3	259.5	12.2	232.5	31.7	154	1.8
	483.3	38.8	452.2	11.5	420.0	35.8	148	1.5
	618.9	51.0	575.0	14.2	536.7	48.6	140	-2.0
	328.9	30.7	301.5	11.0	277.8	30.7	152	-5.8

*Heat Flow Difference T-B = $\dfrac{(\lambda_T) \text{ evaluated using top ref.} - (\lambda_B) \text{ evaluated using bottom ref.}}{\lambda_T + \lambda_B}$ x 200

+Data lost during analysis due to papers being ruined by flood water.

TABLE IIb

Details of Conditions for Each Data Point for Stainless Steel Materials

| Sample | Temperature C | | | | | | λ_T Measured | Heat Flow Difference, %* T-B |
| | Top Heat Meter, T | | Sample | | Bottom Heat Meter, B | | | |
	Mean	ΔT	Mean	ΔT	Mean	ΔT		
0 porosity	+	+	174	19.8	+	+	16.7	4.1
	349.9	24.4	321	21.5	291.1	25.9	19.3	1.3
	618.9	20.9	582	20.7	547.7	23.2	22.8	-2.7
	+	+	891	18.9	+	+	27.1	5.5
	+	+	447	22.7	+	+	21.2	-1.8
9.2 porosity	173.0	18.5	145	22.1	115.0	13.4	12.25	-6.0
	347.3	24.3	311	29.3	272.2	26.1	14.0	2.0
	624.1	19.6	593	26.3	557.9	21.2	16.8	-1.8
	929.6	16.7	898	23.9	867.4	17.8	20.2	-1.6
	360.3	23.7	323	28.8	283.8	26.2	14.4	-0.5
21.38 porosity	174.8	16.7	144	26.8	114	19.1	9.15	-8.6
	388.0	19.6	351	34.2	311	22.9	10.6	-3.8
	765.9	26.8	707	53.9	648.4	30.5	12.7	-1.4
	935.8	16.3	899	34.4	860.5	17.2	13.6	0.8
	555.8	26.8	501	50.7	443.6	32.5	11.6	-8.8
31.0 porosity	241.9	19.2	193	45.5	143.0	21.0	6.2	-4.3
	573.2	23.9	503	68.0	430.5	26.8	7.4	3.1
	804.9	29.0	718	85.5	627	33.7	8.8	0.6
	+	+	893	33.6	+	+	9.2	-7.5
	493.7	20.3	436	55.0	376.0	23.4	7.4	-2.1

*Heat Flow Difference T-B = $\dfrac{(\lambda_T) \text{ evaluated using top ref.} - (\lambda_B) \text{ evaluated using bottom ref.}}{\lambda_T + \lambda_B} \times 200$

+ Data lost during analysis due to papers being ruined by flood water.

TABLE IIc   APPENDIX

DYNATECH CORPORATION   Point # 3   DATA REDUCTION SHEET

Thermal Conductivity by Comparative Method

Temperature Point: ~ 450 C

Sample Designation: Cu 70% Dense

Bottom Heat Meter Material:

Top Heat Meter Material: Armco Iron

Project:

Thickness, X_s : ( ) - ( ) = (1.90)cm

Thickness, X_{BHM}: ( ) - ( ) = (1.90)cm

Thickness, X_{THM}: ( ) - ( ) = (1.90)cm

Thermocouple Material: Avg. of (how many) readings: 4   Data of (date): Sep 9 '70

T/C No	Readings, Mv.	°C
2	3.271	402.1
4	3.615	437.9
6	3.703	446.95
8	3.814	458.45
10	3.917	468.9
12	4.297	507.7

Average Temperatures

BHM   Sample   THM

$$2 \overline{)} \quad 2 \overline{)} \quad 2 \overline{)}$$

420.0   452.2   488.3

Temperature Drops

BHM: 35.8

Sample: 11.5

THM: 38.8

k Heat Meters, watts / cm deg C

BHM: 47.2 @ 420 °C

THM: 43.9 @ 488 °C

$$k_s = k_{HM} \left[\frac{\Delta T_{HM}}{\Delta T_s} \right] \left[\frac{X_s}{X_{HM}} \right]$$

$k_s \Big|_{BHM} = $ $47.2 \times \dfrac{35.8}{11.5} \times \dfrac{1.90}{1.90}$ $k_s \Big|_{THM} = 43.9 \times \dfrac{38.8}{11.5} \times \dfrac{1.90}{1.90}$

$= 147$ $= 149$

Energy Spread

$$200 \frac{k_s \Big|_{BHM} - k_s \Big|_{THM}}{k_s \Big|_{BHM} + k_s \Big|_{THM}} = 1.5 \%$$

$$2 \overline{)}$$

$k_s = 148$ watts / cm deg C @ 452.2 °C

By: HS   Date: Sept 10

DYNATECH CORPORATION

Point #4

DATA REDUCTION SHEET

Thermal Conductivity by Comparative Method

Temperature Point: ~ 900 C

Project:

Sample Designation: S.S 80% porosity

Thickness, X_s : ( ) - ( ) = (1.90)cm

Bottom Heat Meter Material: Inconel 702

Thickness, X_{BHM}: ( ) - ( ) = (1.91)cm

Top Heat Meter Material:

Thickness, X_{THM}: ( ) - ( ) = (1.90)cm

Thermocouple Material: Pt/Pt 10% Rh   Avg. of (how many) readings: 3   Data of (date): 16 Feb '70

T/C No	Readings, Mv.	°C
2	7.897	851.9
4	8.089	869.2
6	8.270	881.9
8	8.615	916.3
10	8.750	928.25
12	8.920	943.25

Average Temperatures

BHM   Sample   THM

$\displaystyle \frac{+}{2 \Big)}$ _____ $\displaystyle \frac{+}{2 \Big)}$ _____ $\displaystyle \frac{+}{2 \Big)}$ _____

860.5   899.1   935.8

Temperature Drops

BHM: 17.3

Sample: 34.4

THM: 15.0

k Heat Meters, watts / cm deg C

BHM: 27.2   @ 860 °C

THM: 29.0   @ 936 °C

$$k_s = k_{HM} \left[\frac{\Delta T_{HM}}{\Delta T_s} \right] \left[\frac{X_s}{X_{HM}} \right]$$

$$k_s \Big|_{BHM} = \quad 27.2 \quad \times \frac{17.3}{34.4} \times \frac{1.90}{1.91} \qquad k_s \Big|_{THM} = 28.9 \times \frac{15.0}{34.4} \times \frac{1.90}{1.90}$$

$$= \quad 13.6 \qquad\qquad = \quad 12.6$$

Energy Spread

$$200 \frac{k_s \Big|_{BHM} - k_s \Big|_{THM}}{k_s \Big|_{BHM} + k_s \Big|_{THM}} = -7.8 \%$$

$\displaystyle \frac{+}{2 \Big)}$ _____

k_s = 13.1   watts / cm deg C @ 899 °C

By: HS   Date: 17 Feb

TABLE III

Collected Results for Thermal Conductivity, λ_T, W m^{-1}deg^{-1}, Electrical Resistivity, ρ, 10^8 Ωm
And Derived Lorenz Number, L, 10^8 V^2 deg K^{-2} for Copper Materials

Nominal Porosity:	0			10			20			30		
Temperature, C	λ_T	$10^8\rho$	10^8L	λ_T	$10^8\rho$	10^8L	λ_T	$10^8\rho$	10^8L	λ_T	$10^8\rho$	10^8L
100	396	2.30	2.44	324	2.85	2.48	232	4.25	2.62	163	6.2	2.62
200	389	3.00	2.47	315	3.70	2.47	221	5.6	2.61	158	7.9	2.64
300	380	3.70	2.45	307	4.55	2.44	207	7.3	2.64	154	9.8	2.64
400	370	4.45	2.44	297.5	5.40	2.39	197	9.0	2.63	148	11.8	2.59
500	360	5.20	2.43	289	6.4	2.40	184	11.15	2.64	143	13.7	2.54
600	351	6.02	2.43	280	7.4	2.37	172	13.1	2.58	139	15.7	2.50
700	342	6.9	2.43	271	8.75	2.44	160	15.1	2.49	-	17.7	-

TABLE IV

Collected Results for Thermal Conductivity, λ_T, W m^{-1}deg^{-1}, Electrical Resistivity, ρ, 10^8 Ωm

And Derived Lorenz Number, L, 10^8 V^2 deg K^{-2} for Stainless Steel

Nominal Porosity:	0			10			20			30		
Temperature, C	λ_T	$10^8\rho$	10^8L	λ_T	$10^8\rho$	10^8L	λ_T	$10^8\rho$	10^8L	λ_T	$10^8\rho$	10^8L
100	16.3	78.8	3.44	11.9	112	3.57	9.1	147.5	3.66	5.5	250	3.69
300	18.9	93.0	3.06	14.0	122	2.99	10.2	175	3.12	6.5	291	3.30
500	21.75	104.5	2.95	16.0	135	2.80	11.4	195	2.88	7.6	315	3.10
700	24.5	112.0	2.82	18.2	146	2.74	12.6	213	2.76	8.6	332	2.93
900	27.3	116.5	2.72	20.4	157	2.72	13.7	231	2.70	9.6	338	2.76

APPLIED PRESSURE
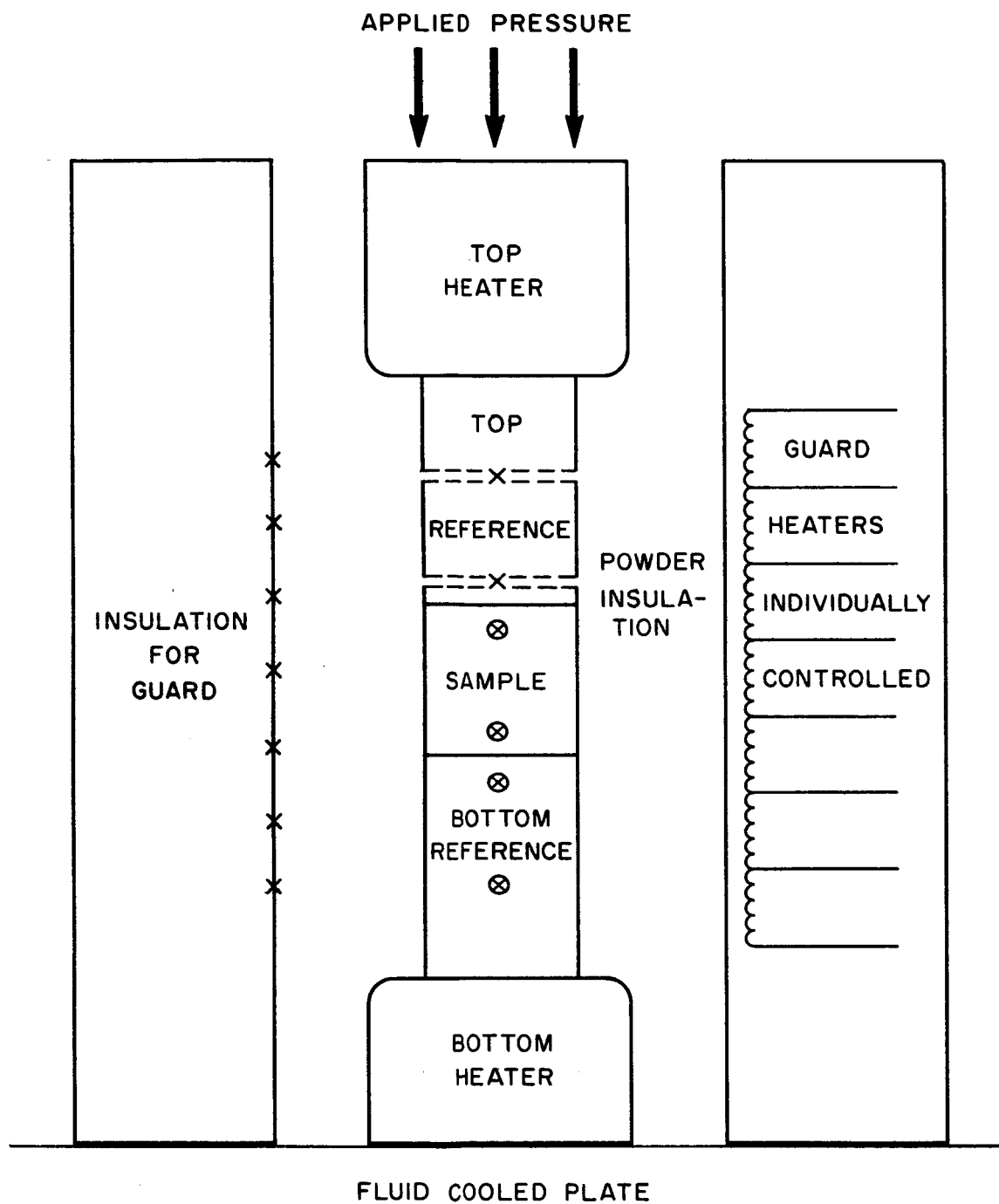
Figure 1. Comparative cut-bar method: schematic assembly.
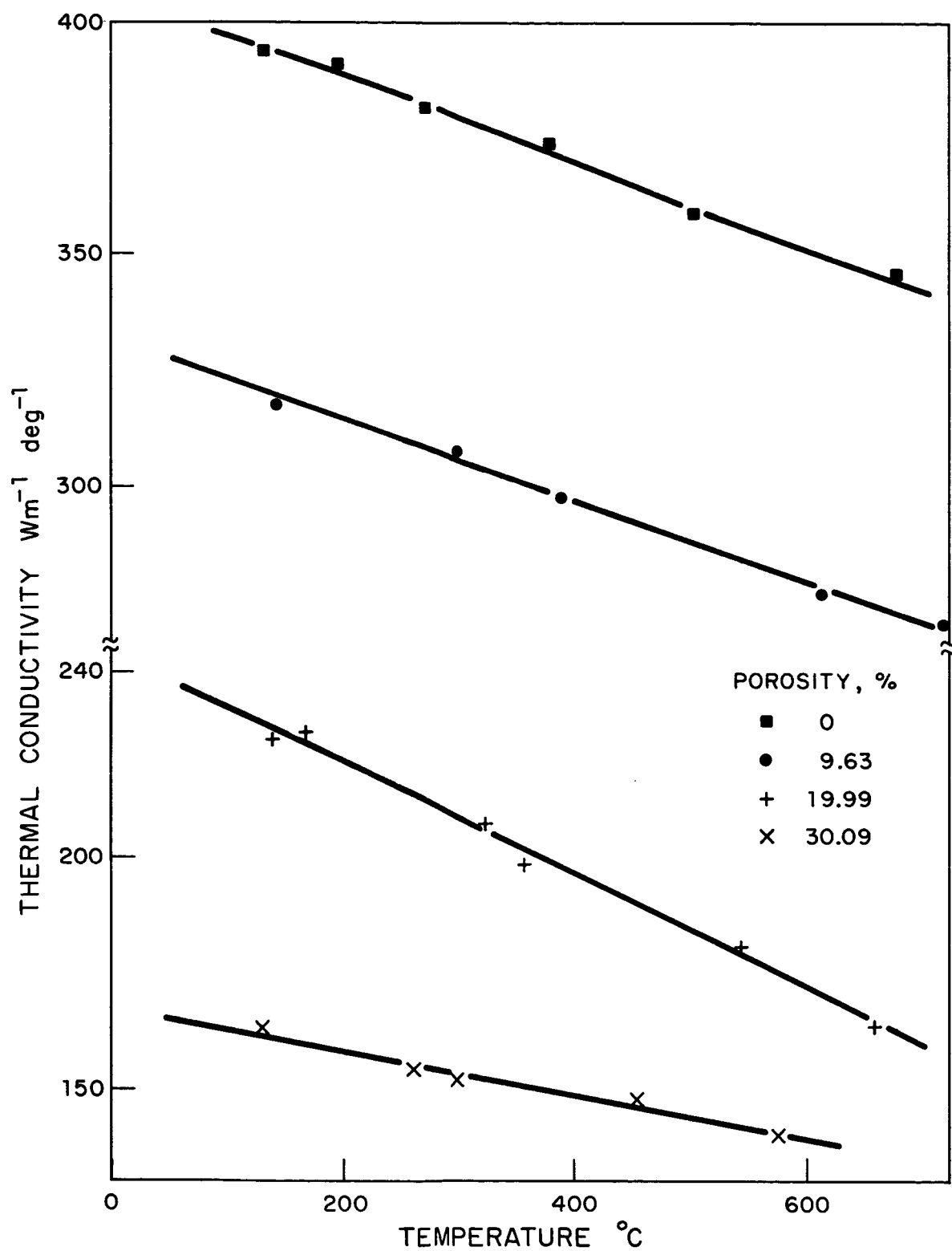X indicates thermocouple positions.

Figure 2a. Thermal conductivity of oxygen free high conductivity copper.
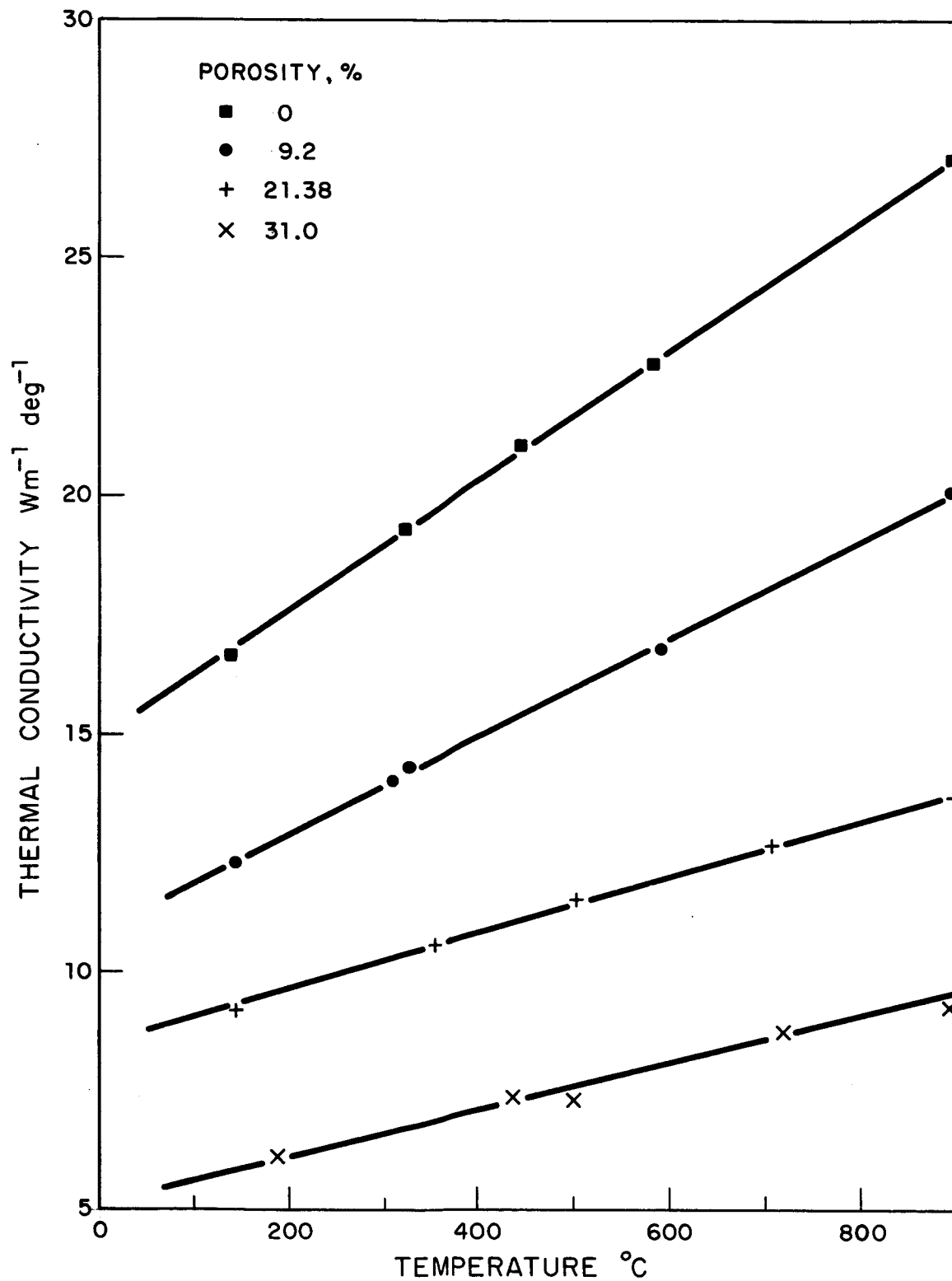
Figure 2b. Thermal conductivity of 304L stainless steel.
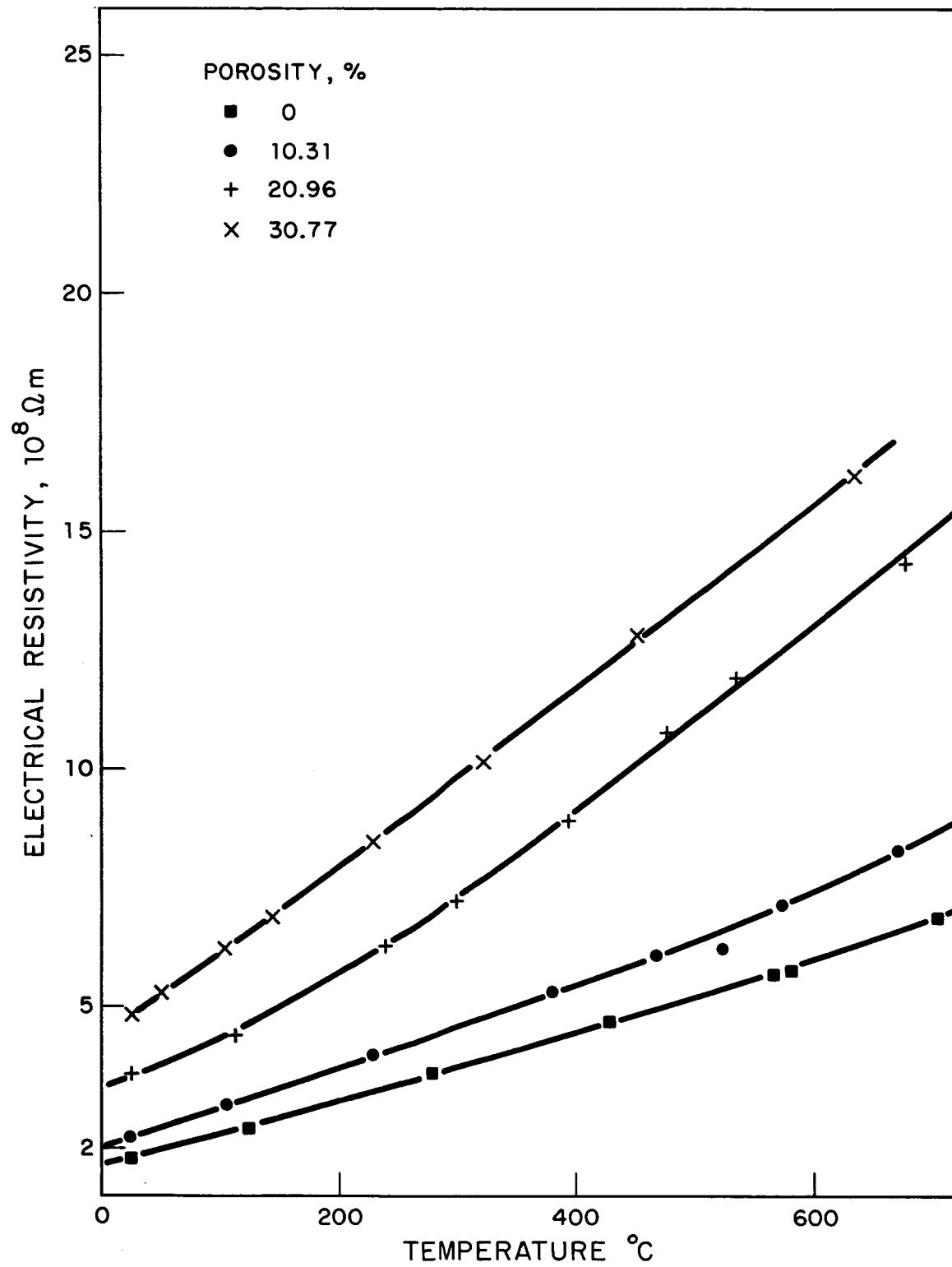
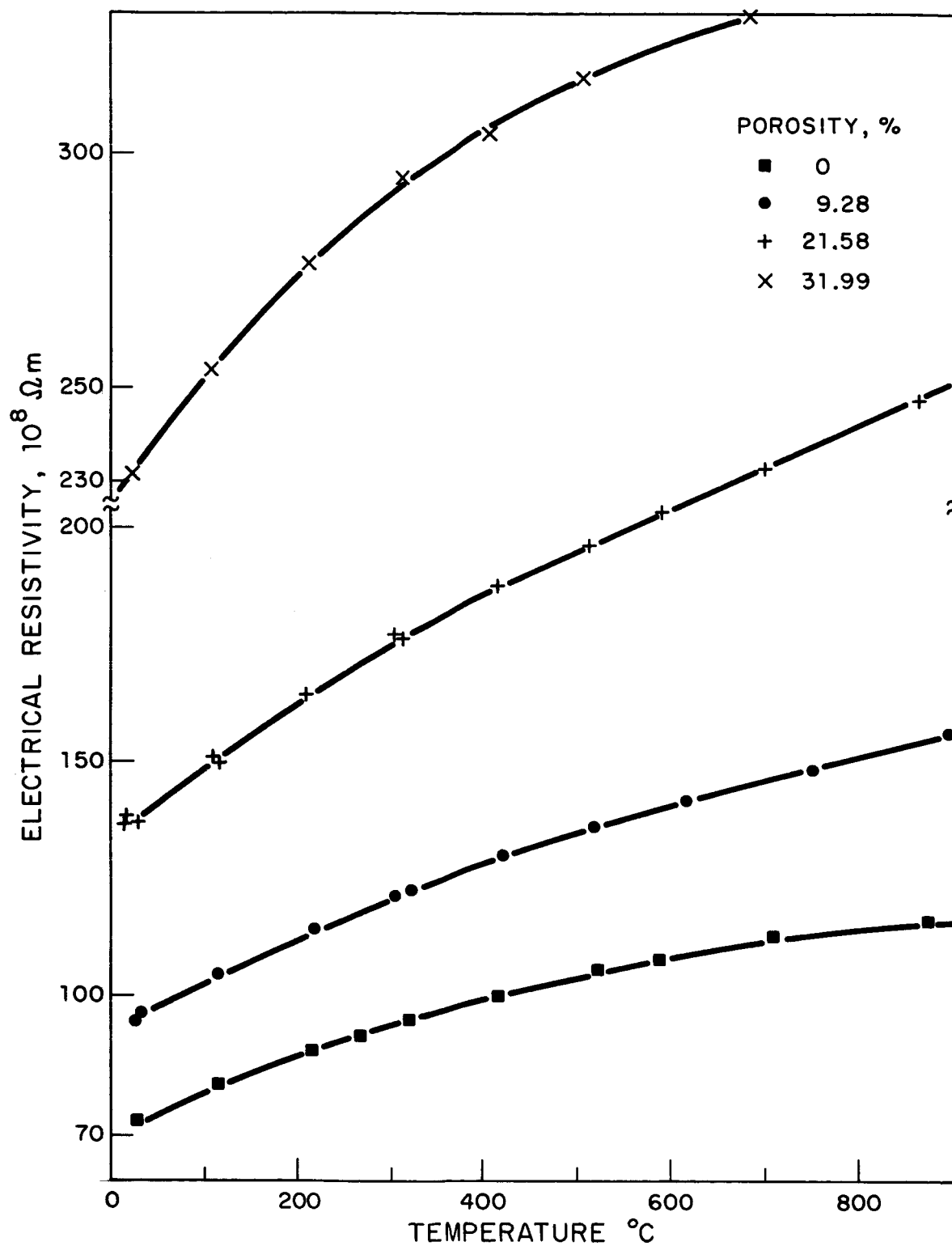Figure 3a. Electrical resistivity of oxygen free high conductivity copper.

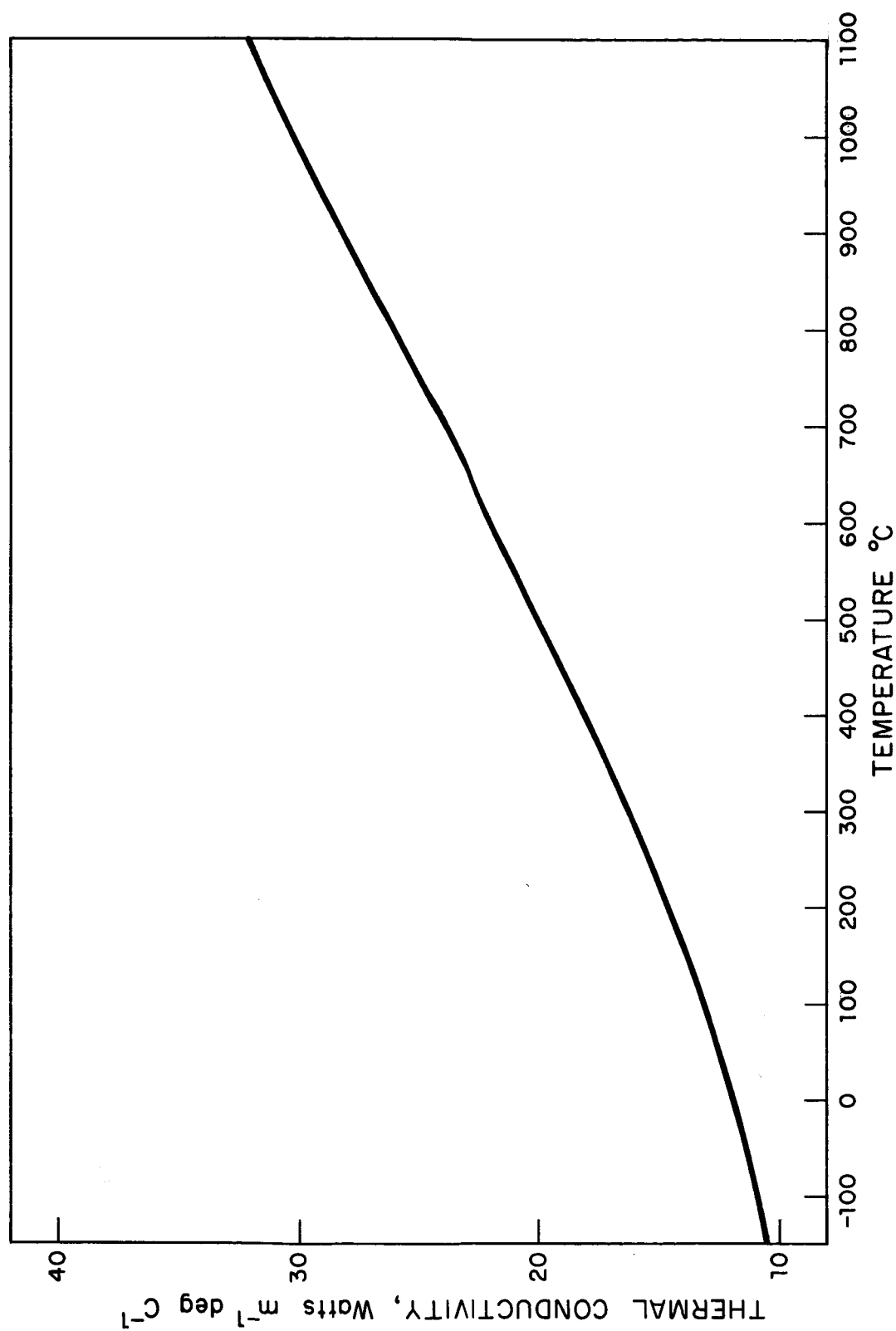Figure 3b. Electrical resistivity of 304L stainless steel.
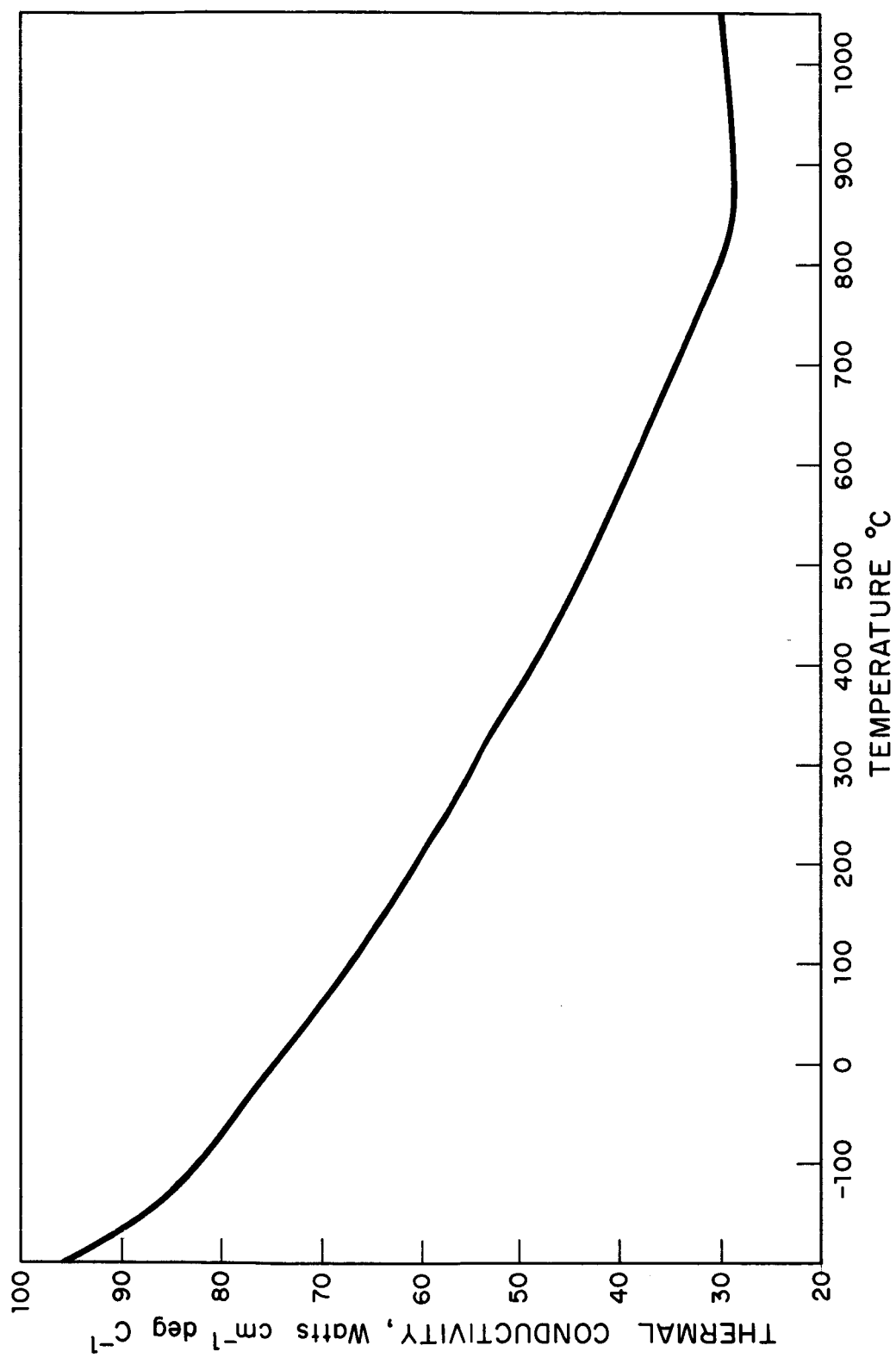
Figure 4. Thermal conductivity of Inconel 702.

Figure 5. Thermal conductivity of Armco Iron.